Energy Reports 12 (2024) 6046–6071

Contents lists available at ScienceDirect

Energy Reports

journal homepage: www.elsevier.com/locate/egyr

Research paper

The life cycle assessment and scenario simulation prediction of intelligent electric vehicles

Yongtao Liu, Qinyang Liu, Longxin Gao, Yunxiang Xing, Yisong Chen *, Shuo Zhang *

School of Automobile, Chang'an University, Xi'an, Shaanxi 710064, PR China

ARTICLE INFO

Keywords:
Intelligent electric vehicles
Life cycle assessment
Scenario simulation
Predictive research

ABSTRACT

Currently, advancements in intelligence, connectivity, and electrification serve as crucial pillars for enhancing traffic efficiency and reducing energy consumption and emissions, with intelligent electric vehicles holding inherent advantages. This study employs life cycle assessment theory to develop models for evaluating the life cycle of intelligent electric and fuel vehicles, covering four stages: raw material acquisition, manufacturing and assembly, operation and use, and end-of-life recycling. This study further investigates the impact of single-vehicle intelligence and vehicle-road coordination technology on the life cycle energy-saving and emission-reduction performance of electric and fuel vehicles in urban and highway scenarios and examines the potential of clean power structures to reduce the energy consumption and emissions of intelligent electric vehicles. The findings indicate that in urban road scenarios, L2-L3 level intelligent electric vehicles with vehicle-road coordination technology reduce life cycle carbon emissions by 20.22 %-22.35 % compared to the L1 level, while fuel vehicles show a reduction of 15.77 %-19.58 %. In highway scenarios, intelligent electric vehicles achieve a reduction of 12.29 %-14.50 %, whereas fuel vehicles show a decrease of 3.47 %-5.91 %. Finally, a life cycle prediction evaluation model was developed to quantitatively forecast and compare the life cycle energy consumption and emissions of intelligent electric and fuel vehicles by 2035. Research indicates that by 2035, the life cycle carbon emissions of intelligent electric vehicles will decrease by 67.81 % compared to 2023 levels, whereas intelligent fuel vehicles will see a reduction of 60.78 %. The life cycle carbon emissions and overall environmental impact potential of intelligent electric vehicles are expected to be reduced by approximately 30 % and 29 %, respectively, compared to intelligent fuel vehicles. These findings provide theoretical and practical guidance for promoting and developing intelligent electric vehicles.

1. Introduction

As sales of new energy vehicles in China continue to rise, intelligent electric vehicles have emerged as one of the most critical subcategories in the automotive industry. China's intelligent electric vehicle industry has experienced continuous growth since 2016, with the market experiencing explosive growth in 2021, 2022, and 2023. By 2025, sales of intelligent electric vehicles are expected to exceed 12.2 million units, comprising 80.1 % of new energy vehicle sales. Intelligent electric vehicles are expected to become the backbone of China's automotive industry in the future.

Life cycle assessment (Hauschild et al., 2018) is the compilation and evaluation of the inputs, outputs, and potential environmental impacts of a product system throughout its entire life cycle. Some scholars (Tagliaferri et al., 2016; Qiao et al., 2017; Zhao et al., 2021; Xia et al., 2022; Verma et al., 2022; Yu et al., 2022; Wang et al., 2023; Song et al., 2023;. Martyushev et al., 2023; Guo et al., 2023) have analyzed the environmental impact of the life cycle of electric vehicles. Some scholars (Ahmadi and Khoshnevisan, 2022; Fu et al., 2023) have used the life cycle assessment method to study the environmental impact of hydrogen fuel vehicles. Some scholars (Wang et al., 2020; Andersson and Börjesson, 2021; Xia et al., 2022; Joshi et al., 2022; Zhang et al., 2023;

Abbreviations: ADPe, Abiotic Depletion Potentialelements; ADPf, Abiotic Depletion Potentialfossil; GWP, Global Warming Potential; AP, Acidification Potential; EP, Eutrophication Potential; POCP, Photochemical Ozone Creation Potential; ODP, Ozone Depletion Potential; LCA, Life Cycle Assessment; LCC, Life Cycle Cost; EV, Electric Vehicle; FCV, Fuel Cell Vehicle; MPC, Model Predictive Control; ACC, Adaptive Cruise Control; ECACC, Ecological Cooperative Adaptive Cruise Control; DA, Driving Assistance; PA, Partial Automation; CA, Conditional Automation; V2G, Vehicle-to-Grid; WLTC, World Light Vehicle Test Cycle.

* Corresponding author.
E-mail addresses: chenyisong_1988@chd.edu.cn (Y. Chen), chenyisong_1988@chd.edu.cn (S. Zhang).

https://doi.org/10.1016/j.egyr.2024.11.056
Received 3 July 2024; Received in revised form 4 November 2024; Accepted 18 November 2024
Available online 4 December 2024

Peng et al., 2023; Chen et al., 2023; Yang et al., 2023; Cui et al., 2023) have studied the energy consumption and greenhouse gas emissions during the life cycle of vehicles with different power sources. Some scholars (Naranjo et al., 2021; Shafique et al., 2022) have used life cycle assessment to analyze the environmental burden of vehicles in different regions, such as Spain and Hong Kong. Some scholars (Lai et al., 2022; Quan et al., 2022) have developed a cradle-to-cradle life cycle assessment framework for different vehicle batteries Some scholars (Sato and Nakata, 2021; Jo and Ahn, 2022; Yang et al., 2022; Jujjavarapu et al., 2023) use the life cycle assessment method to analyze the environmental impact of vehicles and put forward some helpful optimization methods. As a key tool for exploring the environmental impact of vehicles, life cycle assessment demonstrates its depth and breadth in assessing the energy consumption, greenhouse gas emissions, and regional environmental burden of electric vehicles, hydrogen fuel vehicles, and various power source vehicles. Through a detailed analysis of the entire process from production to scrapping, it not only reveals the environmental footprint of vehicles at each stage, but also provides scientific basis for battery technology improvement and overall performance optimization.

In terms of intelligent networking technology, some scholars (Ojeda et al., 2017; Paredes et al., 2019; Cui et al., 2019; Shen et al., 2020; Li et al., 2022; Pan et al., 2022; Zhang et al., 2023) have proposed optimization algorithms for energy efficient driving to solve potential energy waste problems. Some scholars (Guo., 2016, 2019; Chu et al., 2018; Luo., 2020; Bertoni et al., 2017; Jin and Ding, 2018; Jia et al., 2020; Madhusudhanan and Na, 2020; Guo et al., 2021; Yang., 2021; Dong et al., 2021) study and improve adaptive cruise control strategies to reduce vehicle energy consumption and improve environmental benefits. By considering the impact of traffic signals on vehicle speed planning, some scholars (Zheng et al., 2015; Alrifaee et al., 2015; Amini et al., 2019; Wei et al., 2019; Wang and Guo, 2019; Zhang et al., 2019; Liao et al., 2022) can alleviate traffic congestion, improve traffic efficiency, enhance driving safety, and improve vehicle economy. Some scholars (Obaid et al., 2023; Abro et al., 2023) have analyzed the life cycle of autonomous vehicles and pointed out that autonomous driving technology is conducive to improving environmental benefits. Some scholars (Rammohan, 2023; Li et al., 2023; Wang et al., 2021) have analyzed and summarized the necessity of vehicle intelligent network technology, and pointed out that it is conducive to improving vehicle environmental economy. Intelligent networking technology has shown great potential in improving the environmental benefits of vehicles, effectively reducing energy consumption and emissions by optimizing driving modes and traffic management. Scholars' in-depth research has significantly improved traffic efficiency and safety, whether it is innovation in energy-saving algorithms, improvement in adaptive cruise control, or speed planning under the influence of traffic signals. The application of autonomous driving technology further strengthens this trend, not only reducing the environmental burden during the life cycle of vehicles, but also promoting the environmental and economic efficiency of intelligent transportation systems. Intelligent connected technology has become a key driver for achieving green travel and building a sustainable transportation system.

Based on the above analysis, it can be concluded that there has been some research conducted both domestically and internationally on the construction of theoretical models for the full life cycle assessment of electric vehicles, comparative studies on energy conservation and emission reduction of vehicles with different power sources, key factor based full life cycle assessment of electric vehicles, and intelligent vehicle energy-saving scenarios. Quantitative analysis has been conducted on the potential for energy conservation and emission reduction of electric vehicles throughout their entire life cycle, as well as the energy-saving rate under intelligent and networked scenarios. However, there is relatively little research on the impact of intelligence and networking on the resource consumption and environmental emissions of electric vehicles throughout their life cycle. At the same time, there is a lack of comparative analysis and research on the resource consumption and environmental emissions of vehicles with different power sources throughout their life cycle through the implementation of intelligence and networking functions.

This article innovatively applies the full life cycle assessment method to deeply analyze the energy consumption and environmental emissions of intelligent electric vehicles from production to scrapping, and constructs a comprehensive evaluation model of "resource environment cost". By quantifying the energy consumption and emissions under different materials, processes, operating conditions, and energy control strategies, the system identifies key influencing factors such as battery energy density, aiming to explore the energy-saving and emission reduction potential of intelligent electric vehicles. By combining bicycle intelligence, vehicle road collaboration technology, and regional power structure, we simulate the energy efficiency performance of intelligent electric vehicles in multiple scenarios, comprehensively evaluate the deep impact of intelligence, networking, and electrification on energy conservation and emission reduction in the automotive industry, and provide solid theoretical and technical support for building a green automotive industry chain and the high-quality development of the automotive industry. Although this study focuses on in-depth analysis of the life cycle of intelligent vehicles, it does not comprehensively compare their differences in technology and environmental benefits with traditional vehicles. Recognizing the limitations of this research, we hope that future studies can further explore the comparative analysis between intelligent vehicles and traditional vehicles based on this research, in order to gain a comprehensive understanding of the all-round value of intelligent vehicles.

2. Methodology

2.1. Evaluation methods

This study utilizes the CML2001 evaluation method to characterize and standardize the consumption of mineral resources, fossil energy, carbon emissions, and pollutant emissions from the model output. The focus is on two types of energy consumption and five types of environmental impacts. ADP(e) and ADP(f) are employed to measure the life cycle consumption of mineral resources and fossil energy for intelligent electric vehicles. The GWP was used to represent carbon emissions, whereas AP, EP, POCP, and ODP were used to comprehensively assess pollutant emissions. Life cycle costs are considered to evaluate the economic performance of vehicles.

With the continuous development and improvement of life cycle assessment methods in various fields, there are more than 30 modeling software dedicated to life cycle assessment, including GaBi, SimaPro, GREET, Umbeato, eBalance, etc., both domestically and internationally. Each software contains a large number of directly usable databases, such as upstream preparation and downstream scrap recycling lists for nonmetallic materials such as plastics, rubber, glass, as well as metal materials such as steel, iron, copper, and aluminum. It also includes data lists for primary and secondary energy sources such as electricity, petroleum, and thermal energy. Among them, GaBi has the richest and most comprehensive data list for automobiles in the current market, with a database covering a large amount of Sphera data as well as association and industry data that is continuously updated. This article chooses GaBi software to evaluate and study the energy-saving and emission reduction performance of intelligent electric vehicles and intelligent fuel vehicles.

2.2. System boundaries

In this study, the life cycle assessment of intelligent electric vehicles was divided into four stages: raw material acquisition, manufacturing and assembly, operation and use, and end-of-life recycling. The system boundary diagram is shown in Fig. 1. For system inputs, this study primarily considers various fossil fuels, including crude oil, hard coal, and

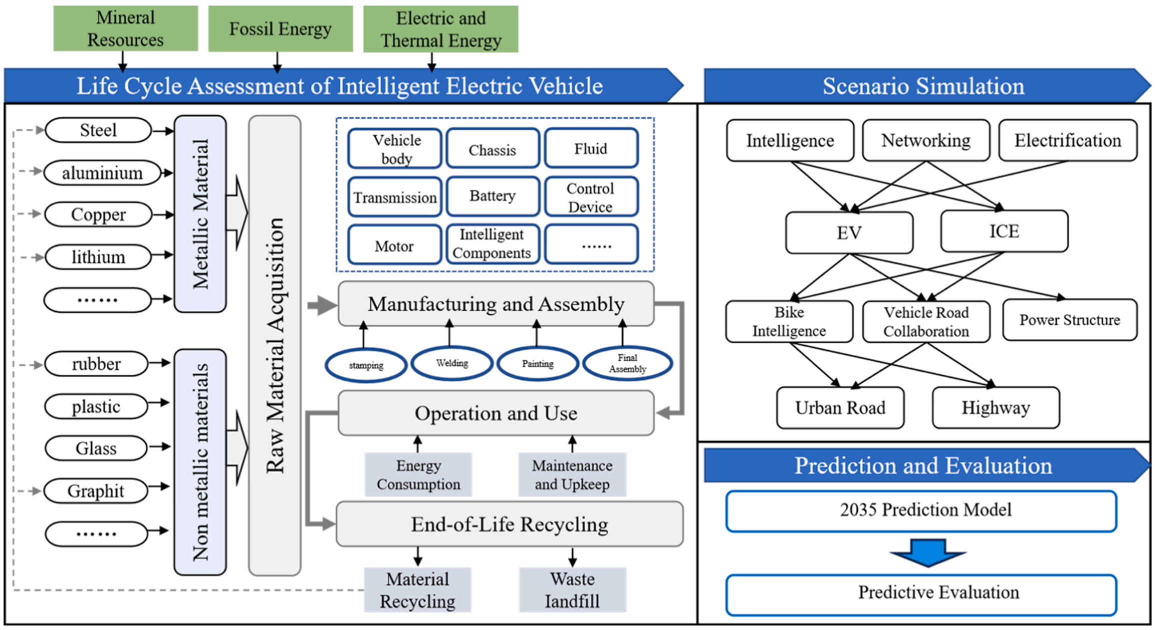

Fig. 1. The system boundary.

natural gas, as well as essential mineral resources such as steel, aluminum, iron, and copper. For the output parameters, the focus was on measuring the GWP of greenhouse gas emissions, while also considering other pollutant emissions, such as the AP, EP, POCP, and ODP. The raw material acquisition stage focuses on collecting, organizing, and dynamically analyzing data on the key components of intelligent electric vehicles. These components include the body, power battery, chassis, electronic control devices, main reducer, electric motor, intelligent network components (such as the onboard radar, cameras, and sensors), and fluids and liquids. This stage covers a detailed inventory of metallic and non-metallic materials. In the manufacturing and assembly stages, emphasis is placed on the energy input required to produce the aforementioned components, primarily electricity and thermal energy consumption. It also considers the energy consumption and environmental emissions during vehicle assembly. In the operation and use stage, the primary considerations are electric energy consumption, energy consumption, and environmental emissions during the upstream preparation and transportation processes. In the end-of-life recycling stage, the positive environmental benefits of reusing key components and recyclable materials are considered, as well as the negative environmental impacts of landfill and incineration processes. Components with lighter weights or minimal impacts on the overall evaluation results are not discussed in detail in this study.

A functional unit refers to the quantified performance of the product system, which is used as the baseline unit. According to the "Technical Specification for Accounting of Passenger Car Life Cycle Carbon Emissions" released by the China Automotive Technology and Research Center, the life cycle mileage is calculated as 1.5 × 10ˆ5 km when accounting for the life cycle energy consumption and emissions of passenger cars.

2.3. Calculation model

Based on the life cycle assessment theory and the previously constructed system boundaries for intelligent electric vehicles, this study established resource depletion evaluation models (divided into mineral resources and fossil energy) and environmental emission evaluation models (divided into carbon emissions and pollutant emissions) for four stages: raw material acquisition, manufacturing and assembly, operation and use, and end-of-life recycling.

2.3.1. Resource depletion

The consumption of mineral resources during the raw material acquisition stage mainly originates from two parts. The first part involves the conversion of mineral resources into metal materials such as steel, iron, and copper, as well as non-metal materials such as plastics and rubber through processes such as processing and smelting. The second is the loss generated during the machining of basic raw materials into automotive components through procedures such as planning, milling, grinding, and turning. Fossil energy consumption refers to the use of secondary energy sources such as gasoline, diesel, and electricity during the aforementioned processes. The mineral resource consumption matrix during the raw material acquisition stage is given by Eq. (1):

$$M_{rma} = \sum_{n}\left[(m_{ij})_{n\times k}\cdot(\varepsilon_{ij})_{k\times m}\cdot\theta^{-1}\right] \tag{1}$$

where m_{ij} represents the mass of the j kind of vehicle raw material contained in the i kind of automobile parts, n represents the number of auto parts, k represents the number of types of vehicle materials, ε_{ij} represents the amount of the j kind of mineral resources required to produce the i kind of vehicle material, m represents the number of types of mineral resources, where $\theta = diag\{\theta_{11}, \theta_{22}, \dots, \theta_{kk}\}$, and θ_{ij} represents the processing utilization of the j kind of vehicle material when processing auto parts.

The fossil energy consumption matrix during the raw material acquisition stage is given by Eq. (2):

$$F_{rma} = \sum_{n} \left(M_{rma}\cdot E_2\cdot E_1 \right) \tag{2}$$

where $E_1 = (e_{1ij})_{q\times p}$ represents the unit energy consumption matrix of energy production, where e_{1ij} represents the j primary energy quantity consumed by the i secondary energy of the production unit, p represents the number of types of primary energy, q represents the number of types of secondary energy; $E_2 = (e_{2ij})_{m\times q}$ represents the energy consumption intensity matrix of the raw material production stage, and e_{2ij} represents the j secondary energy quantity consumed by the production of the i vehicle material.

The manufacturing and assembly stage primarily involves processing automotive materials into components and completing assembly on the production line. This process incurs almost no material loss, considering only the energy consumption generated by each procedure. The fossil energy consumption matrix during the manufacturing and assembly stage is given by Eq. (3):

$$F_{man} = \sum_{n} E_3 \cdot E_1 \tag{3}$$

where $E_3 = (e_{3ij})_{n\times q}$, e_{3ij} denotes the amount of secondary energy of type j required to produce and complete the assembly of type i parts.

During the operation and use stage of intelligent electric vehicles, the consumption of electric energy and the replacement of some components, such as tires, are considered. The mineral resource consumption matrix during the operation and use stage is given by Eq. (4):

$$M_{use} = \sum_{n} \delta_i [(m_{ij})_{n\times k} \cdot (\varepsilon_{ij})_{k\times m} \cdot \theta^{-1}] \tag{4}$$

where δ_i represents the number of replacement of the part i that needs to be replaced.

The fossil energy consumption matrix during the operation and use stage is given by Eq. (5):

$$F_{use} = Q \times \frac{\frac{L}{100}}{\gamma} \cdot (e_{1j})_{1\times q} \cdot E_1 \tag{5}$$

where Q represents the power consumption of intelligent electric vehicle for *100* kilometers *[kWh (100 km) −1]*, L represents the driving range of the whole life cycle, γrepresents the utilization efficiency of electric energy, and e_{1j} represents the j type secondary energy quantity needed to produce unit electric energy.

In the scrapping and recycling stage, the emphasis is on the reuse of intelligent devices (sensors, cameras, and radars) and the recycling of metallic materials such as steel, cast iron, and aluminum, as well as non-metallic materials such as rubber. The mineral resource consumption matrix during the scrapping and recycling stage is given by Eq. (6):

$$M_{rec} = -\sum_{n} \mu_i [(m_{ij})_{n\times k'} \cdot (\varepsilon_{ij})_{k'\times m} \cdot \theta^{-1}] \tag{6}$$

where k'represents the number of types of recyclable material, and μ_i indicates the recycling rate of the i type recyclable material.

The fossil energy consumption matrix during the end-of-life recycling stage is given by Eq. (7):

$$F_{rec} = \sum_{n} M_{rec} \cdot (E_4 - E_2) \cdot E_1 \tag{7}$$

where $E_4 = (e_{4ij})_{m\times q}$, e_{4ij} represents the amount of the j type of secondary energy consumed to recover the i type of vehicle material.

2.3.2. Environmental emissions

The life cycle environmental emissions of intelligent electric vehicles primarily refer to the gas emissions and organic outputs generated during material acquisition, component manufacturing and assembly, and electric energy production throughout their life cycle. To examine the benefits of intelligent electric vehicles in reducing carbon emissions more intuitively, this study divides the environmental emission evaluation model into carbon and pollutant emission evaluation models and calculates them based on the previously constructed resource depletion evaluation model.

Environmental emissions during the raw material acquisition stage mainly originate from smelting and other processes involved in obtaining automotive materials as well as the extraction and combustion of fossil fuels such as coal and oil. The carbon emission matrix during the raw material acquisition stage is given by Eq. (8):

$$C_{rma} = \sum_{n} [(m_{ij})_{n\times k} \cdot (c_{1ij})_{k\times 1}] \tag{8}$$

where c_{1ij} represents the carbon emission equivalent ($kg \cdot kg^{-1}$) produced by the production of the i type vehicle material per unit mass.

The pollutant emission matrix during the raw material acquisition stage is given by Eq. (9):

$$P_{rma} = \sum_{n} [(m_{ij})_{n\times k} \cdot (p_{1ij})_{k\times h}] \tag{9}$$

where p_{1ij} represents the emission equivalent ($kg \cdot kg^{-1}$) of the j type pollutant produced per unit mass of the i type vehicle material, and h represents the number of types of pollutants discharged.

Environmental emissions during the manufacturing and assembly stage primarily originate from the upstream acquisition of electric and thermal energy consumed during component manufacturing and assembly. The carbon emission matrix during the manufacturing and assembly stage is given by Eq. (10):

$$C_{man} = \sum_{n} [F_{man} \cdot (c_{0ij})_{p\times 1}] \tag{10}$$

where c_{0ij} represents the carbon emission equivalent (kg/MJ) produced by the i type primary energy source per unit of mass.

The pollutant emission matrix during the manufacturing and assembly stage is shown in Eq. (11):

$$P_{man} = \sum_{n} [F_{man} \cdot (p_{0ij})_{p\times h}] \tag{11}$$

where p_{0ij} represents the pollutant emission equivalent (kg/MJ) produced by the production of the i type first primary energy of unit mass.

The carbon emission matrix during the operation and use stage is given by Eq. (12):

$$C_{use} = \sum_{n} [\delta_i (m_{ij})_{n\times k} \cdot \theta^{-1} \cdot (c_{1ij})_{k\times 1} + F_{use} \cdot (c_{0ij})_{p\times 1}] \tag{12}$$

The pollutant emission matrix during the operation and use stage is shown in Eq. (13):

$$P_{use} = \sum_{n} [\delta_i (m_{ij})_{n\times k} \cdot \theta^{-1} \cdot (p_{1ij})_{k\times h} + F_{use} \cdot (p_{0ij})_{p\times h}] \tag{13}$$

The carbon emission matrix during the end-of-life recycling stage is given by Eq. (14):

$$C_{rec} = \sum_{n} [-\mu_i (m_{ij})_{n\times k'} \cdot \theta^{-1} \cdot (c_{1ij})_{k'\times 1} + F_{rec} \cdot (c_{0ij})_{p\times 1}] \tag{14}$$

The pollutant emission matrix during the end-of-life recycling stage is given by Eq. (15):

$$P_{rec} = \sum_{n} [-\mu_i (m_{ij})_{n\times k'} \cdot \theta^{-1} \cdot (p_{1ij})_{k'\times h} + F_{rec} \cdot (p_{0ij})_{p\times h}] \tag{15}$$

2.3.3. Cost evaluation

LCC refers to the total cost incurred throughout the entire life cycle of a product, including raw material acquisition, product usage costs, and other expenses, as shown in Table 1.

To align the cost estimation results with consumer needs, this study constructed a life cycle cost evaluation model for intelligent electric vehicles from the consumer perspective, considering the system boundaries of the research object. The main considerations include vehicle purchase, operation and use, and end-of-life recycling costs, as shown in Eq. (16):

$$C_{LCA} = C_1 + C_2 - C_3 \tag{16}$$

where C_1 represents the vehicle purchase cost (*ten thousand yuan*), mainly including the vehicle purchase price, purchase tax, government subsidy, insurance, and other expenses; C_2 represents the operation and use cost, mainly considering the power consumption cost of the vehicle, as shown in Eq. (17); C_3 represents the residual value of the vehicle scrap recovery (*ten thousand yuan*).

Table 1
Life cycle cost components under multiple perspectives.

Stage	Business Cost	Consumer Cost	Social Cost
Design	Feasibility and Market Research, Design, Testing, Redesign, etc.	-	-
Manufacturing	Raw Materials, Equipment, Wages, etc.	-	Wastewater/ Gas, Solid Waste
Sales Selling	Expenses, Bonuses, Advertising Costs, Transportation Fees, etc.	Purchase Cost, Acquisition Tax	-
Operational Maintenance	Post-sale Maintenance and Repairs	Energy Consumption, Repair and Maintenance, Insurance Premiums	Wastewater/ Gas,Solid Waste
End-of-Life Disposal	-	Disposal Cost, Residual Value	Wastewater/ Gas,Solid Waste

$$C_2 = \sum_{i=1}^{n}[\frac{S_i}{100} \times H \times P_i + C_i^B + C_i^S] \times \frac{1}{(1+q)^{i-1}} \tag{17}$$

where S_i represents the running mileage (*km*) of the *i* year, H represents the power consumption of the vehicle for *100* km [$kWh\ (100\ km)^{-1}$], P_i means the average price of the *i* year (*ten thousand yuan/kWh*), C_i^B represents the repair cost of the vehicle in the *i* year (*ten thousand yuan*), C_i^S represents the maintenance cost of the vehicle in the *i* year (*ten thousand yuan*), and q indicates the discount rate.

2.4. Prediction model

Based on the life cycle assessment theoretical model constructed earlier, a vehicle life cycle prediction evaluation model was developed, considering key factors such as the power structure, vehicle lightweight coefficient, and fuel/electricity consumption per 100 km.

The life cycle mineral resource consumption prediction matrix is given by Eq. (18).

$$M_{LCA} = \gamma\cdot(M_{rma} + M_{use} + M_{rec}) + M'_{rec} \tag{18}$$

where $\gamma = diag\{\gamma_{11}, \gamma_{22}, \cdots, \gamma_{nn}\}$, γ_{ij} represents the lightweight factor of each component of the vehicle; M_{rma} represents the mineral resource consumption matrix of the raw material stage of acquisition, M_{use} represents the mineral resource consumption matrix of the operation and use stage, M_{rec} represents the mineral resource consumption matrix in the scrap recovery stage; M'_{rec} represents the supplementary material consumption matrix of the vehicle scrap recovery stage, focusing on the scrap recycling of power battery.

The life cycle fossil energy consumption prediction matrix is given by Eq. (19):

$$F_{LCA} = \gamma\cdot(F_{rma} + F_{rec}) + F'_{man} + (1-\rho)F_{use} \tag{19}$$

In ρ says the hundreds of kilometers of power consumption, F_{rma} said raw material acquisition stage of fossil energy consumption matrix, F_{rec} said scrap recycling stage fossil energy consumption matrix, F_{use} represents the operation stage fossil energy consumption matrix, F'_{man} said as the vehicle parts lightweight after manufacturing assembly stage of fossil energy consumption matrix.

The life cycle carbon emission prediction matrix is shown in Eq. (20):

$$C_{LCA} = M_{LCA}\cdot(c_{2ij})_{m\times 1} + F_{LCA}\cdot(c_{0ij})_{p\times 1} \tag{20}$$

where c_{2ij} represents carbon emissions from the production of the i-th mineral resource.

The life cycle pollutant emission prediction matrix is shown in Eq. (21):

$$P_{LCA} = M_{LCA}\cdot\left(p_{2ij}\right)_{m\times 1} + F_{LCA}\cdot\left(p_{0ij}\right)_{p\times h} \tag{21}$$

where p_{2ij} represents the discharge of the j-th pollutant produced during the production of the ith mineral resources.

3. Data inventory and evaluation results

3.1. Data inventory

To enhance the comparability between intelligent electric vehicles and intelligent fuel vehicles, this study comprehensively considers factors such as vehicle class, wheelbase, curb weight, maximum power, maximum torque, and intelligence level, selecting the Audi A6L as the research object. The basic parameter comparison table of intelligent electric vehicles and intelligent fuel vehicles is presented in Table 2.

3.1.1. Raw material acquisition

The raw material acquisition stage refers to the processing of material resources into automotive raw materials. This study divides intelligent electric vehicles into eight parts: body, chassis, main reducer, power battery, electric motor, electronic control devices, fluids and liquids, and intelligent components (onboard radar, cameras, and sensors). Based on the literature review and field investigation, the mass and proportion of each part relative to the curb weight are listed in Table 3. The data inventory of the intelligent electric vehicles is presented in Table 4.

As the power source of electric vehicles, power batteries are the most important system in the vehicle, accounting for about 30–40 % of the cost of the vehicle. At present, there are two mainstream battery technology routes for electric vehicles: lithium iron phosphate battery and terre lithium battery. Lithium iron phosphate battery has the characteristics of safety, long life and high temperature resistance, and terre lithium battery has the advantages of light weight, high charging efficiency and low temperature resistance. Many scholars (Lai et al., 2022; Quan et al., 2022) also studied the life-cycle effects of both.

The research object selected in this paper is equipped with a lithium iron phosphate battery with a capacity of 85.44kWh. According to the official website, the energy density of this battery is 150 Wh/kg, and the mass of the lithium iron phosphate battery of this research object is calculated to be 569.6 kg. In the research process, the lithium iron phosphate battery is divided into positive electrode, negative electrode, adhesive, diaphragm, electrolyte, coolant, BMS and shell eight parts, through comparative study of domestic and foreign literature, develop a detailed list.

Intelligent fuel vehicles are mainly divided into seven parts: engine,

Table 2
Comparison of basic parameters of intelligent electric vehicle and intelligent fuel vehicle.

Parameter Name	Intelligent Electric Vehicle	Intelligent Fuel Vehicle
Length×Width×Height/ mm×mm×mm	4995 × 1910 × 1495	5050 × 1886 × 1475
Curb Weight/kg	2100	1810
Wheelbase /mm	2920	3024
Max Torque/N·m	350	370
Top Speed/km^{-1}	185	230
Peak Engine Power/kW	-	180
Combined System Power/kW	180	-
Energy Consumption per 100 km/kWh·100 km^{-1}	13.5	-
Fuel Consumption per 100 km/ L·100 km^{-1}	-	7.18
Intelligence Level	L2	L2

Table 3
Quality of each part and its proportion to the quality of the service (Yang et al., 2022; Chen et al., 2023; Song et al., 2023).

Component Name	Mass/kg	Percentage/%
Body	718.2	34.2
Chassis	556.5	26.5
Main Reducer	44.1	2.1
Power Battery	569.6	27.1
Electric Motor	94.5	4.5
Electrical Control Unit	79.8	3.8
Smart Connectivity Components	10.5	0.5
Fluids and Liquids	27.3	1.3

transmission, body, chassis, fluids, battery, and intelligent components, with mass proportions of 10.10 %, 8.40 %, 42 %, 38.50 %, 1.90 %, 1.30 %, and 0.5 %, respectively. To ensure the comparability of the research results, the manufacturing and assembly stage of intelligent fuel vehicles only considers the consumption of electric and thermal energy. The material proportions and manufacturing energy consumption of each component of intelligent fuel vehicles are listed in Table 5.

3.1.2. Manufacturing and assembly

The manufacturing and assembly stage of intelligent electric vehicles mainly includes four component manufacturing and assembly processes: stamping, welding, painting, and final assembly. The energy consumption and environmental impact at this stage mainly originate from the electric and thermal energy consumed by these four processes, as well as some materials. Based on the literature and field investigations, the energy consumption of the major components during the manufacturing stage of intelligent electric vehicles is presented in Table 6.

3.1.3. Operation and use

The energy consumption and environmental emissions during the operation phase of intelligent electric vehicles primarily stem from electricity consumption and vehicle maintenance, including the regular replacement of fluids, liquids, tires, and other easily worn parts. According to the literature (Meng et al., 2022), intelligent electric vehicles require tire replacements every 61,500 km, amounting to two replacements over their entire life cycle. Based on typical vehicle maintenance cycles, the lubricating oil was replaced every 6250 km, totaling 23 replacements throughout the life cycle. The wiper fluid was completely consumed every 12,500 km, necessitating 11 replacements over its entire life cycle. The brake fluid and coolant were replaced every 62,500 km, each requiring two replacements over its life cycle. Lithium iron phosphate batteries can endure more than 2000 charging cycles and, based on a life cycle mileage of 150,000 km, do not require replacement during the vehicle life cycle.

Regarding energy consumption, the subject of this study had a maximum power output of 180 kW and a power consumption rate of 13.5 kWh per 100 km. Considering factors such as charging/discharging efficiency and battery energy degradation, and assuming a 90 % charging/discharging efficiency, the total life-cycle energy consumption is $2.25 \times 10\hat{}4$ kWh.

Energy consumption and emissions during the operational phase of intelligent fuel vehicles primarily originate from gasoline production and combustion, as well as vehicle maintenance. To ensure the comparability of the research results, the functional unit was set at 150,000 km, with the frequency of lubricant and wiper fluid replacements aligned with intelligent electric vehicles. Based on China's standards for "Limits and Measurement Methods for Emissions from Light-Duty Vehicles (Stage VI)" and literature research, the pollutant emissions per unit volume of gasoline over its life cycle were calculated using the CML2001 method via GaBi software, as shown in Table 7.

3.1.4. End-of-life recycling

The end-of-life recycling stage of intelligent electric vehicles primarily considers the negative environmental impacts of energy consumption required for processes such as dismantling and shredding after the vehicle is scrapped, as well as the positive environmental impacts of reusing some of the recovered materials. This study divides the end-of-life recycling stage into two main parts. The first part involves

Table 4
Data list of intelligent electric vehicles.

Component Name	Material Name	Percentage	Reference	Component Name	Material Name	Percentage	Reference
Body	Steel	68.70 %	(Chen et al., 2023; Liu., 2016)	Electric Motor	Copper	16 %	(Zhou., 2016; Ding et al., 2021)
	Aluminum	0.80 %			Steel	31.60 %	
	Copper	1.90 %			Neodymium Iron Boron	13.20 %	
	Magnesium	0.04 %			Aluminum Alloy	39.20 %	
	Plastic	17.40 %		Lithium Iron Phosphate Battery	Lithium Iron Phosphate	24.38 %	(Hao et al., 2017;Hao., 2023)
	Fiberglass	6.60 %			Aluminum	20.30 %	
	Rubber	0.51 %			Polyvinylidene Fluoride	1.05 %	
	Other	4.05 %			Graphite	15.20 %	
Chassis	Steel	82.30 %	(Chen et al., 2023; Liu., 2016)		Copper	12.40 %	
	Cast Iron	6.30 %			Lithium Hexafluorophosphate	2.70 %	
	Aluminum	1 %			Ethylene Carbonate	7.80 %	
	Copper	2.30 %			Dimethyl Ester	7.80 %	
	Plastic	3.30 %			Polypropylene	3.20 %	
	Rubber	4.20 %			Steel	1.50 %	
	Other	0.60 %			Polyethylene	0.30 %	
Final Drive	Steel	60.50 %	(Chen et al., 2023; Liu., 2016)		Ethylene Glycol	1.00 %	
	Aluminum	20 %					
	Copper	19 %			Others	2.00 %	
	Plastic	0.50 %		Fluids and Liquids	Lubricating Oil	3.17 %	(Ma., 2019)
Electronic Control Unit	Aluminum	47 %	(Li., 2015; Ma., 2019)		Brake Fluid	3.58 %	
	Steel	5 %			Coolant	28.58 %	
	Thermoplastic	3.70 %			Windshield Washer Fluid	10.71 %	
	Plastic	23.80 %			Adhesive	53.96 %	
	Copper	8.20 %					
	Organic Material	12.30 %					

Note 1: The list of Polytetrafluoroethene is not available in GaBi database and replaced by high strength polyethylene;
Note 2: In neodymium iron boron, neodymium accounts for 29.1 %, iron accounts for 69.7 %, and boron accounts for 10 %. In addition, producing 1 kg of neodymium iron boron requires 9.1kWh of electricity and 3.37 kg of hard coal (Liu and Xu, 2016)

Table 5
Material proportion and manufacturing energy consumption of each component of intelligent fuel vehicle (Fu et al. 2023; Chen et al. 2023).

Component	Material Composition	Electrical Energy Consumption/ MJ•kg^{-1}	thermal Energy Consumption/ MJ•kg^{-1}	Mass Percentage
Engine	1 % Copper, 35.7 % Steel, 4.5 % Plastic, 42 % Aluminum, 12.3 % Cast Iron, 4.5 % Rubber	11.02	-	10.10 %
Transmission	30 % Steel, 30 % Aluminum, 30 % Cast Iron, 5 % Rubber, 5 % Plastic	17.97	10.7	8.40 %
Body	1.93 % Copper, 17.4 % Plastic, 0.77 % Forged Aluminum, 6.6 % Glass, 0.04 % Magnesium, 68.7 % Steel, 0.51 % Rubber, 4.05 % Others	3.43	-	42 %
Chassis	82.3 % Steel, 6.3 % Iron, 1 % Aluminum, 2.3 % Copper, 3.3 % Plastic, 4.2 % Rubber, 0.6 % Others	1.39	0.43	35.80 %
Hydraulics	10.71 % Windshield Washer Fluid, 3.17 % Lubricating Oil, 28.58 % Coolant, 3.58 % Brake Fluid, 53.96 % Adhesive	66.92	-	1.90 %
Battery	Battery 6.1 % Polypropylene, 69.0 % Lead, 14.1 % Water, 7.9 % Sulfuric Acid, 2.1 % Glass Fiber, 0.8 % Others	2.72	-	1.30 %

recycling of traditional component materials, such as the body and chassis, focusing on the recovery of aluminum, iron, copper, steel, and rubber. The second part is the end-of-life recycling of lithium iron phosphate batteries. Current recycling technologies for lithium iron phosphate batteries are mainly divided into cascade utilization and regeneration. This study primarily refers to a new "physical method" for recycling all components, which first discharges waste batteries and then performs precise automated disassembly to separate and recover the metal and plastic components. Subsequently, the anode and cathode of the battery cells were disassembled, crushed, and sorted to obtain copper, aluminum, and electrode material powders. Finally, according to the literature (Wang, 2018), the recovered cathode material powder was optimized using material restoration technology and re-synthesized into a new cathode material through high-temperature reactions, achieving the partial recycling of waste lithium iron phosphate batteries. The energy consumption and recycling efficiency of various automotive materials and lithium iron phosphate batteries are presented in Table 8.

3.2. Evaluation results

Based on the inventory data of intelligent fuel vehicles, the full life cycle assessment results for intelligent fuel vehicles in 2023 were obtained using the full life cycle predictive evaluation model and CML2001 evaluation method, as shown in Table 9. The data analysis revealed that the full life cycle ADP(e), ADP(f), GWP, AP, EP, POCP, and ODP of intelligent fuel vehicles in 2023 are 4.31E-02, 4.78E+ 05, 3.83E+ 04, 4.61E+ 01, 6.09E+ 00, 1.24E+ 01, and 6.16E-08 kg, respectively. Compared to intelligent electric vehicles in the same period, the ADP(e), AP, EP, and ODP of intelligent fuel vehicles decreased by 51.46 %, 31.09 %, 17.14 %, and 75.94 %, respectively. ADP(f), GWP, and POCP increased by 70.11 %, 32.53 %, and 183.75 %, respectively, as shown in Fig. 2.

Table 8
Energy consumption and recovery efficiency of automotive materials and lithium iron phosphate battery recycling (Chen et al., 2023; Wang., 2018).

Type	Recycled Materials (Component Name)	Preprocessing Energy Consumption /kWh·kg^{-1}	Recycling Efficiency (Recovered Mass per Unit Weight)
Automotive Materials	Steel	4.23	75 %
	Aluminum	0.8	87 %
	Copper	9.54	90 %
	Iron	2.24	80 %
	Rubber	-	37 %
Lithium Iron Phosphate Battery	Graphite	12.4	0.100
	Aluminum Foil		0.177
	Copper		0.116

Table 6
Energy consumption in manufacturing process of main components of intelligent electric vehicles (Chen et al., 2023, 2022; Song et al., 2023; Hao., 2023;).

Energy Consumption Type	Body	Chassis	Main Reducer	Lithium Iron Phosphate Battery	Electric Motor	Electrical Control System	Hydraulics and Fluids
Electrical Energy Consumption/ MJ•kg^{-1}	3.43	1.39	6.93	11.7	5.28	1.38	66.92
Thermal Energy Consumption/ MJ•kg^{-1}	-	0.42	4.14	8.8	1.9	-	-

Table 7
Life cycle energy consumption and emission of gasoline per unit volume.

Stage	ADP(f)/MJ·L^{-1}	GWP/kg·L^{-1}	AP/kg·L^{-1}	EP/kg·L^{-1}	POCP/kg·L^{-1}	ODP/kg·L^{-1}
Petroleum Refining	3.61E+ 01	4.06E−01	2.08E−03	2.35E−04	4.75E−04	3.27E−13
Gasoline Combustion	-	2.42E+ 00	5.09E−04	1.32E−04	5.41E−04	-
Life Cycle Assessment	3.61E+ 01	2.83E+ 00	2.59E−03	3.67E−04	1.02E−03	3.27E−13

Table 9
Full life cycle evaluation results of intelligent electric vehicles and intelligent fuel vehicles in 2023.

Vehicle	Type	ADP(e)/kg	ADP(f)/MJ	GWP/kg	AP/kg	EP/kg	POCP/kg	ODP/kg
Intelligent Electric Vehicle	I	4.53E−01	9.87E+ 04	1.21E+ 04	4.91E+ 01	2.47E+ 00	3.91E+ 00	2.12E−08
	II	6.90E−04	6.30E+ 04	5.99E+ 03	1.26E+ 01	1.72E+ 00	8.03E−01	5.36E−08
	III	2.08E−03	1.62E+ 05	1.51E+ 04	3.17E+ 01	4.35E+ 00	2.05E+ 00	1.61E−07
	IV	−3.67E−01	−4.28E+ 04	−4.25E+ 03	−2.65E+ 01	−1.19E+ 00	−2.39E+ 00	2.02E−08
	Total	8.88E−02	2.81E+ 05	2.89E+ 04	6.69E+ 01	7.35E+ 00	4.37E+ 00	2.56E−07
Intelligent Fuel Vehicle	I	1.23E−01	7.38E+ 04	6.76E+ 03	2.50E+ 01	1.73E+ 00	2.62E+ 00	4.06E−09
	II	5.87E−04	5.07E+ 04	4.82E+ 03	1.01E+ 01	1.38E+ 00	6.46E−01	4.57E−08
	III	1.86E−03	3.94E+ 05	3.06E+ 04	2.81E+ 01	4.01E+ 00	1.10E+ 01	3.85E−09
	IV	−8.29E−02	−4.05E+ 04	−3.96E+ 03	−1.71E+ 01	−1.04E+ 00	−1.86E+ 00	8.01E−09
	Total	4.31E−02	4.78E+ 05	3.83E+ 04	4.61E+ 01	6.09E+ 00	1.24E+ 01	6.16E−08

Note: I represents the Raw Material Acquisition stage, II represents the Manufacturing and Assembly stage, III represents the Operation and Use stage, IV represents the End-of-Life Recycling stage, and the Total represents Life Cycle Assessment.

3.3. Cost evaluation

Due to the fact that intelligent electric vehicles are an emerging technology, their cost-benefit analysis may have more research value and urgency, which can help promote industry decision-making and policy-making. Therefore, only the cost analysis of intelligent electric vehicles has been conducted.

According to the whole life cycle cost model of intelligent electric vehicles constructed above, the acquisition cost, operation cost and scrap recovery cost of intelligent electric vehicles are collected through literature research and field investigation. The cost composition table is shown in Table 10. According to the analysis of Table 10, the total life cycle cost of the intelligent electric vehicle studied in this paper is 318,100 yuan, of which the vehicle acquisition cost is the highest, and the operation and use stage cost only accounts for 9 % of the total life cycle cost. Therefore, without considering the replacement of core components such as batteries, compared with traditional fuel vehicles, The cost advantage of the whole life cycle of intelligent electric vehicles is obvious. In addition, taking Fujian Province as an example, the charging peak, peak, flat and low period of time are 2 hours, 6 hours, 8 hours, 8 hours, respectively, and the electricity price is 1.04 yuan, 0.95 yuan, 0.67 yuan, 0.41 yuan per KWH of electricity. The charging fee for the corresponding period is 52.1 yuan, 47.6 yuan, 33.9 yuan and 20.3 yuan respectively, and the difference between the trough and the peak period is 31.9 yuan. Therefore, promoting the charging of electric vehicles in the off-peak hours of the power system and improving the utilization efficiency of the power system will help reduce the cost of intelligent electric vehicles.

Table 10
Full life cycle cost of intelligent electric vehicles.

Cost Composition	**Specific Content**	**Amount/Ten Thousand Yuan**
Purchase Cost	Selling Price	23.98
	Purchase Tax	0
	National Government Subsidy	0[1]
	Insurance Expense	3.29[2]
	Total	27.27
Operation and Use Cost	Power Consumption Cost	1.55[3]
	Maintenance Cost	1.32[4]
	Total	2.87
End-of-Life Recycling Cost	-	−1.2
Life Cycle Cost	-	31.81

Note 1: The Ministry of Finance, the Ministry of Industry and Information Technology, the Ministry of Science and Technology and the Development and Reform Commission jointly issued the Notice on the Financial Subsidy Policy for the Promotion and Application of New energy Vehicles in 2022, pointing out that vehicles registered after December 31, 2022 will no longer be subsidized;
Note 2: The insurance cost consists of RMB950 for compulsory traffic insurance and RMB3170 for commercial insurance;
Note 3: Electric vehicle charging is divided into two kinds: home charging pile and commercial charging pile, and the price is not uniform in different regions. In this paper, the average price of charging is about 0.69 yuan /kWh based on the peak-valley TOU price policy of Fujian Province.
Note 4: According to the data provided by the White Paper on the Maintenance Industry of Passenger Vehicles in the Automobile Aftermarket of Tongji University, the average unit price and unit price of maintenance customers of new energy vehicles in China are 1329 yuan and 193 yuan, and the average annual maintenance times of the full sample vehicles are about 1.9 times, which are calculated according to the life of new energy vehicles for 8 years and the first 4 years of warranty without maintenance.

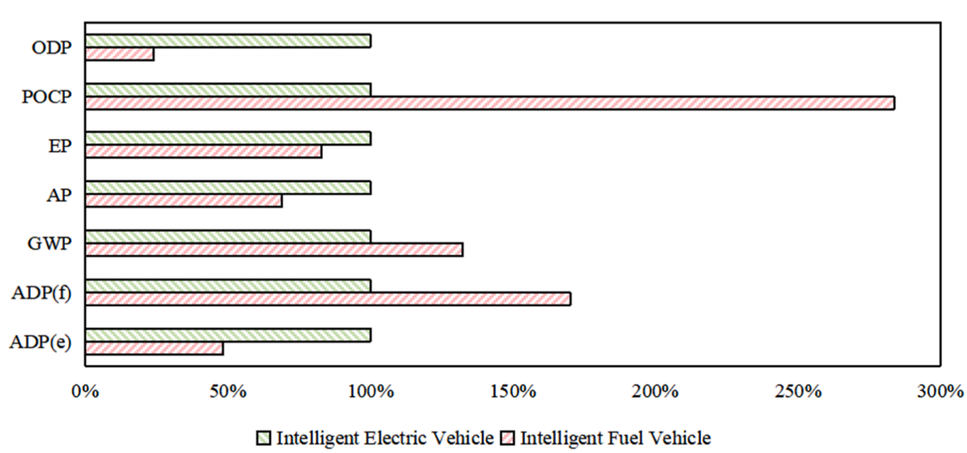

Fig. 2. Changes in energy consumption and emissions of intelligent electric vehicles throughout their life cycle in 2023.

4. Multi-scenario simulation study

4.1. Scenario simulation study on single vehicle intelligence coupled with multiple operating scenarios

4.1.1. Single vehicle intelligence scenario setup

The intelligent electric vehicles studied in this paper essentially combine intelligent connected vehicles and electric vehicles, equipped with power batteries for electric drive, and fitted with human-vehicle interaction intelligent cockpits or L2-level and above intelligent driving functions. Considering the current maturity of single vehicle intelligence technology, this study primarily focused on intelligent electric vehicles with L1 and L2-L3 levels of single-vehicle intelligence, corresponding to DA and PA/CA in China's intelligent driving classification. In the development of intelligent electric vehicles, the functions of intelligent driving are divided into two categories–driving and parking–based on the different attributes, application algorithms, and decision algorithms of the research subjects during high-speed driving and low-speed parking. According to the function and scenario system of intelligent driving, there are currently seven mainstream driving functions and five parking functions corresponding to the L1-L4 levels of intelligence and different functional performances. Among them, based on different available areas, navigation-assisted driving is mainly divided into high-speed navigation assistance and urban navigation assistance. Owing to technical limitations, current mass-produced navigation-assisted driving systems are all high-speed navigation assistance systems, whereas urban road navigation assistance functions have not yet been fully developed. From the perspective of the scenario system, common operating scenarios for intelligent electric vehicles include three main areas: highways, urban areas, and parking lots. Highways and urban areas were the driving scenarios, and parking lots were the parking scenarios. Based on the above research, this section primarily considers the full life cycle energy consumption, carbon emissions, and pollutant emissions of L1-level electric vehicles and fuel vehicles, as well as L2-L3-level intelligent electric vehicles and intelligent fuel vehicles, in the two major driving scenarios of highways and urban road. (((Table 11)))

Considering the impact of different algorithms and target parameter settings on the energy-saving rate, we conducted simulation test experiments based on the literature. Utilizing the university's automobile test field, the energy-saving efficiency of intelligent electric vehicles in autonomous driving mode under urban and highway scenarios is measured and verified, as shown in Fig. 3.

Based on the aforementioned research, this study established eight different scenario settings comprising two levels of single vehicle intelligence, two types of vehicles, and two operational scenarios, as illustrated in Table 12. Particular emphasis is placed on how variations in electricity and fuel consumption during the operational phase affect energy consumption and carbon and pollutant emissions.

4.1.2. Analysis of results for single vehicle intelligence

By applying the constructed scenarios to the previously developed vehicle life cycle assessment model, we obtained the energy consumption, carbon emissions, and pollutant emissions for intelligent fuel vehicles and intelligent electric vehicles with different levels of single vehicle intelligence during the operational phase in the urban and highway scenarios, as shown in Table 13. Because different levels of single vehicle intelligence have a minimal impact on resource consumption and environmental emissions during the raw material acquisition, manufacturing, and disposal stages, this study focused solely on the changes during the operational phase for the two vehicle types. The life cycle assessment results are presented in Table 14.

The analysis of Fig. 4 indicates that in urban road scenarios, the full life cycle fossil energy consumption of L2-L3 level electric vehicles is reduced by 14.60 % compared to the L1 level, whereas for fuel vehicles, the reduction is 7.99 %. The fossil energy consumption of L1 level

Table 11
Intelligent Classification Standards for Single Vehicles.

Driving Control Applicable Scenarios	Level	Driving Function	Parking Function
-	L1	ACC (Adaptive Cruise Control) stands for Adaptive Cruise Control. By identifying the target vehicle ahead through vehicle sensors, cruise control is achieved based on the set target speed and inter vehicle time interval: if there is no vehicle ahead, it enters a constant speed cruise control state. ALC (Auto Lane Change) stands for Automatic Lane Change Assist. During vehicle operation, remind the driver to change lanes while ensuring safety. After confirmation by the driver, assist the driver in executing the lane change action. LCC (Lane Centering Control) refers to lane centering control. LCC is a pure lateral control function that automatically maintains the vehicle in the center of the lane through recognition of lane markings and automatic control of the steering system.	-
ICA (Intelligence Cruise Assist) stands for Intelligent Navigation Assistance. Integrated TJA and HWA functions.	L2	TJA (Traffic Jam Assistant) stands for Traffic Jam Assistance. The traffic congestion assistance system (low-speed) combines adaptive cruise control system with automatic following function, as well as lane keeping assistance system. HWA (Highway Assist) stands for High Speed Driving Assistance. High speed driving assistance (highway) combines adaptive cruise control system with automatic following function, as well as lane keeping assistance system.	APA (Auto Parking Assist) stands for Automatic Parking Assist function. After the function is turned on, APA recognizes the available parking spaces around the vehicle, and after the driver selects a parking space, controls the vehicle's horizontal and vertical movements to achieve automatic parking in and out of the parking space. RPA (Remote Parking Assist) stands for Remote Parking Assist. After getting off the car, the driver controls the vehicle to automatically park in and out of the parking space through remote control methods such as mobile apps.
NGP (Navigation Guided Pilot) refers to automatic navigation assisted driving. Integrating	L3	TJP (Traffic Jam Pilot) stands for Traffic Jam Pilot. Add navigation and automatic lane merging on the basis of	SS (Smart Summon) refers to the intelligent summoning function. Car owners can issue call commands outside

(continued on next page)

Table 11 (*continued*)

Driving Control Applicable Scenarios	Level	Driving Function	Parking Function
TIP and HWP functions.		TJA. HWP (Highway Pilot) stands for High Speed Driving Guidance. Add high-speed navigation, automatic merging, and automatic ramp up and down on the basis of HWA.	the car through a mobile app to control the vehicle's automatic movement and reach the designated location. HPA (Home zone Parking Assist) stands for Memory Parking Function. Through self-learning of the system, HPA can remember the specific parking spaces and driving trajectories of vehicles in a specific area (home or company parking lot), and control the vehicles to automatically complete all actions of finding and parking spaces from the entrance of the parking lot.
-	L4	-	AVP (Automated Valet Parking) stands for Autonomous Valet Parking. AVP is truly autonomous driving, where vehicles can enter completely unfamiliar parking lots on their own without the need for prior learning, and can complete all parking actions without the need for the driver to be in the car.

electric vehicles was 55.66 % lower than that of fuel vehicles of the same level, and for L2-L3 levels, the reduction was 58.85 %. In the highway scenario, the full life cycle fossil energy consumption of L2-L3 level electric vehicles is reduced by only 9.81 % compared to the L1 level, whereas for fuel vehicles, the reduction is 4.03 %. The fossil energy consumption of L1 level electric vehicles was 24.23 % lower than that of fuel vehicles of the same level, and for L2-L3 levels, the reduction was 28.78 %. In summary, enhancing the level of single vehicle intelligence has the potential to reduce the full life cycle fossil energy consumption of both electric and fuel vehicles, with a more significant reduction observed in urban road scenarios. Furthermore, as the level of single vehicle intelligence increases, the reduction in fossil energy consumption of electric vehicles compared to fuel vehicles of the same level becomes increasingly significant.

The analysis of Fig. 5 shows that in the urban road scenario, the full life cycle carbon emissions of L2-L3 level electric vehicles are reduced by 13.40 % compared to the L1 level, whereas for fuel vehicles, the reduction is 7.80 %. The carbon emissions of L1 level electric vehicles were 43.1 % lower than those of fuel vehicles of the same level, and for the L2-L3 levels, the reduction was 46.56 %. In the highway scenario, the full life cycle carbon emissions of L2-L3 level electric vehicles are reduced by only 9.13 % compared to the L1 level, whereas for fuel vehicles, the reduction is 3.98 %. The carbon emissions of L1 level electric

Table 12
Scenarios of coupling multiple running scenarios with two different intelligence levels(Guo., 2016; Chu et al., 2018; Luo., 2020; Bertoni et al., 2017; Jin and Ding, 2018; Guo., 2019; Jia et al., 2020; Madhusudhanan and Na, 2020; Guo et al., 2021; Yang., 2021; Dong et al., 2021).

Vehicle Type	Autonomous Level	Operating Scenario	Energy Saving Rate	Power Consumption per 100 km/kWh Fuel Consumption per 100 km/L
Intelligent Electric Vehicle	L1	Urban Road	-	17
		Highway	-	20
	L2-L3	Urban Road	25 %	13
		Highway	15 %	17
Intelligent Fuel Vehicle	L1	Urban Road	-	11.8
		Highway	-	7.1
	L2-L3	Urban Road	8 %	10.7
		Highway	5 %	6.7

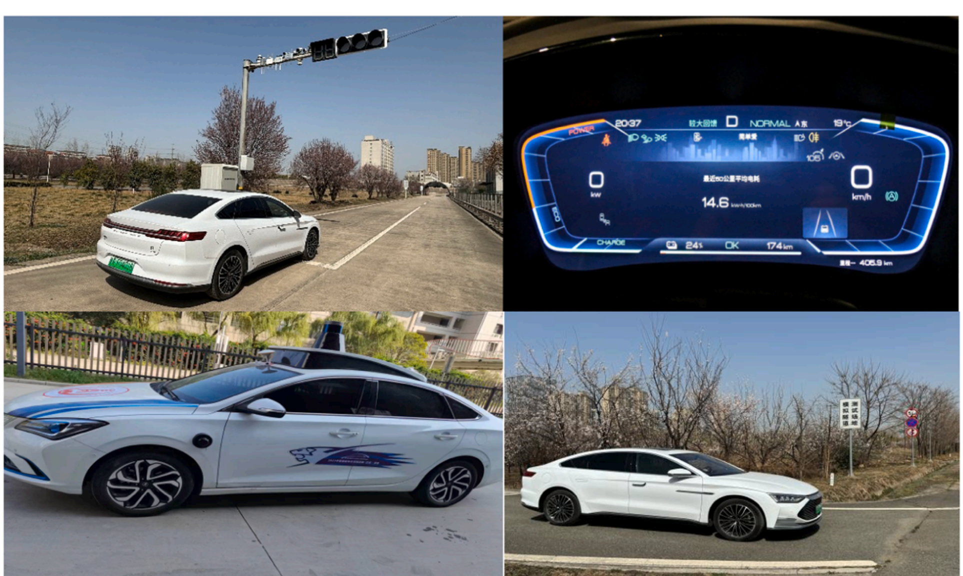

Fig. 3. Simulation experiment of test site.

Table 13
Evaluation results of the operation and use stage of the intelligent coupling multi-operation scenarios for two types of vehicles.

Operating Scenario	Vehicle Type	Vehicle Autonomous Level	ADP(f)/MJ	GWP/kg	AP/kg	EP/kg	POCP/kg	ODP/kg
Urban Road	Intelligent Electric Vehicle	L1	2.03E+ 05	1.90E+ 04	3.99E+ 01	5.46E+ 00	2.02E−07	2.57E+ 00
		L2-L3	1.56E+ 05	1.46E+ 04	3.06E+ 01	4.19E+ 00	1.55E−07	1.97E+ 00
	Intelligent Fuel Vehicle	L1	6.42E+ 05	5.01E+ 04	4.59E+ 01	6.54E+ 00	6.09E−09	1.80E+ 01
		L2-L3	5.84E+ 05	4.56E+ 04	4.18E+ 01	5.95E+ 00	5.58E−09	1.63E+ 01
Highway	Intelligent Electric Vehicle	L1	2.38E+ 05	2.23E+ 04	4.69E+ 01	6.42E+ 00	2.38E−07	3.02E+ 00
		L2-L3	2.03E+ 05	1.90E+ 04	3.99E+ 01	5.46E+ 00	2.02E−07	2.57E+ 00
	Intelligent Fuel Vehicle	L1	3.87E+ 05	3.01E+ 04	2.76E+ 01	3.94E+ 00	3.79E−09	1.08E+ 01
		L2-L3	3.68E+ 05	2.86E+ 04	2.63E+ 01	3.75E+ 00	3.62E−09	1.03E+ 01

Table 14
Full life cycle evaluation results of intelligent coupling multi-operation scenarios for two vehicle types.

Operating Scenario	Vehicle Type	Vehicle Autonomous Level	ADP(f)/MJ	GWP/kg	AP/kg	EP/kg	POCP/kg	ODP/kg
Urban Road	Intelligent Electric Vehicle	L1	3.22E+ 05	3.28E+ 04	7.51E+ 01	8.46E+ 00	2.97E−07	4.89E+ 00
		L2-L3	2.75E+ 05	2.84E+ 04	6.58E+ 01	7.19E+ 00	2.50E−07	4.29E+ 00
	Intelligent Fuel Vehicle	L1	7.26E+ 05	5.77E+ 04	6.39E+ 01	8.61E+ 00	6.39E−08	1.94E+ 01
		L2-L3	6.68E+ 05	5.32E+ 04	5.98E+ 01	8.02E+ 00	6.34E−08	1.77E+ 01
Highway	Intelligent Electric Vehicle	L1	3.57E+ 05	3.61E+ 04	8.21E+ 01	9.42E+ 00	3.33E−07	5.34E+ 00
		L2-L3	3.22E+ 05	3.28E+ 04	7.51E+ 01	8.46E+ 00	2.97E−07	4.89E+ 00
	Intelligent Fuel Vehicle	L1	4.71E+ 05	3.77E+ 04	4.56E+ 01	6.01E+ 00	6.16E−08	1.22E+ 01
		L2-L3	4.52E+ 05	3.62E+ 04	4.43E+ 01	5.82E+ 00	6.14E−08	1.17E+ 01

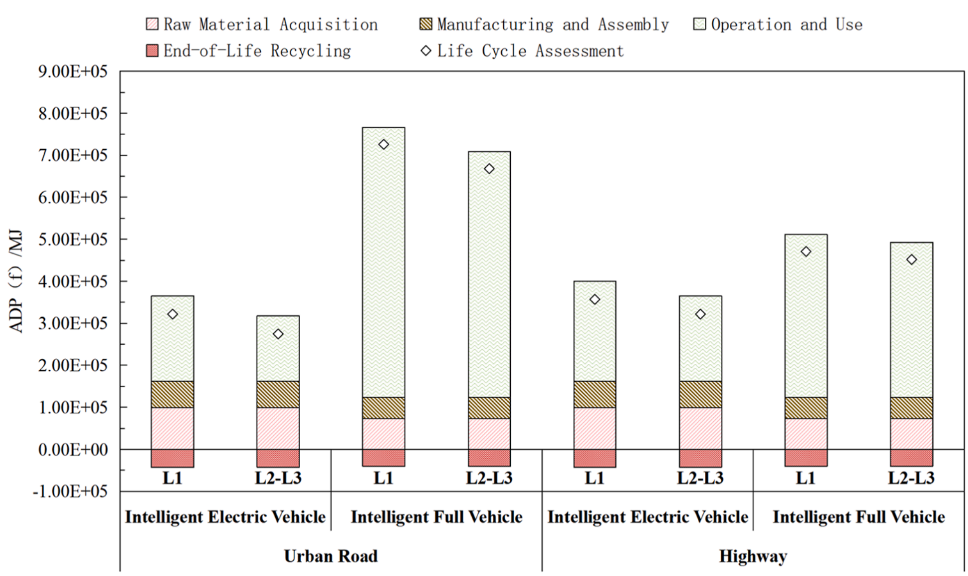

Fig. 4. Full life cycle of intelligent coupling multi-operation scenarios of two models ADP(f).

vehicles were 24.19 % lower than those of fuel vehicles of the same level, and for L2-L3 levels, the reduction was 28.33 %. In summary, enhancing the level of single vehicle intelligence has the potential to reduce the full life cycle carbon emissions of both electric and fuel vehicles, with a more significant reduction observed in urban road scenarios. Furthermore, as the level of single vehicle intelligence increases, the reduction in carbon emissions of electric vehicles compared to fuel vehicles of the same level becomes increasingly significant.

The analysis of Fig. 6 indicates that in urban road scenarios, the life cycle of L2-L3 electric vehicles' AP, EP, POCP, and ODP decreased by 12.38 %, 15.01 %, 12.26 %, and 15.82 %, respectively, compared to L1. In contrast, fuel vehicles showed decreases of 6.42 %, 6.85 %, 8.76 %, and 0.80 %, respectively. For L1 electric vehicles, AP and ODP increased compared with their fuel counterparts, whereas EP and POCP decreased. For L2-L3 electric vehicles, the AP, EP, and ODP increased, whereas the POCP decreased. However, as the level of intelligence increases, the rate of change also increases. In the highway scenarios, the life cycle AP, EP, POCP, and ODP of L2-L3 electric vehicles decreased by 8.53 %, 10.19 %, 8.42 %, and 10.81 %, respectively, compared to L1. For fuel vehicles, the decreases were 2.85 %, 3.16 %, 4.10 %, and 0.28 %, respectively. The trends in AP, EP, POCP, and ODP changes for L1 and L2-L3 electric vehicles compared to those of their fuel counterparts were similar. In summary, increasing the level of vehicle intelligence has the potential to reduce the life cycle pollutant emissions of both electric and fuel vehicles, with greater reductions observed in urban road scenarios. Additionally, as the level of vehicle intelligence increases, the disparity in pollutant emissions between electric and fuel vehicles gradually narrows.

4.2. Scenario simulation study on vehicle-road coordination in multiple operating scenarios

4.2.1. Setting the vehicle-road coordination scenarios

Vehicle-road coordination builds on single-vehicle intelligent autonomous driving technology, relying on advanced vehicles and smart roads for real-time, high-precision traffic environment monitoring and

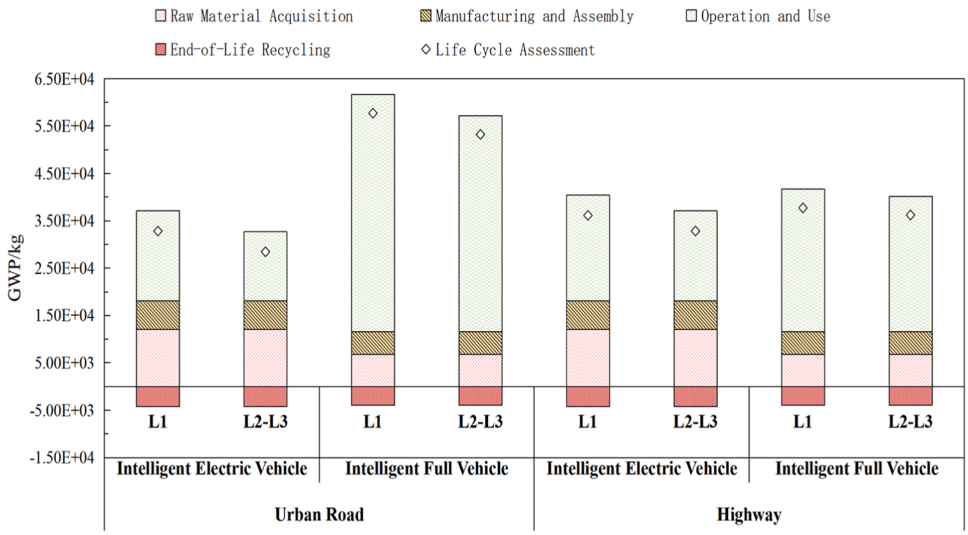

Fig. 5. Full life cycle of intelligent coupling multi-operation scenarios of two models GWP.

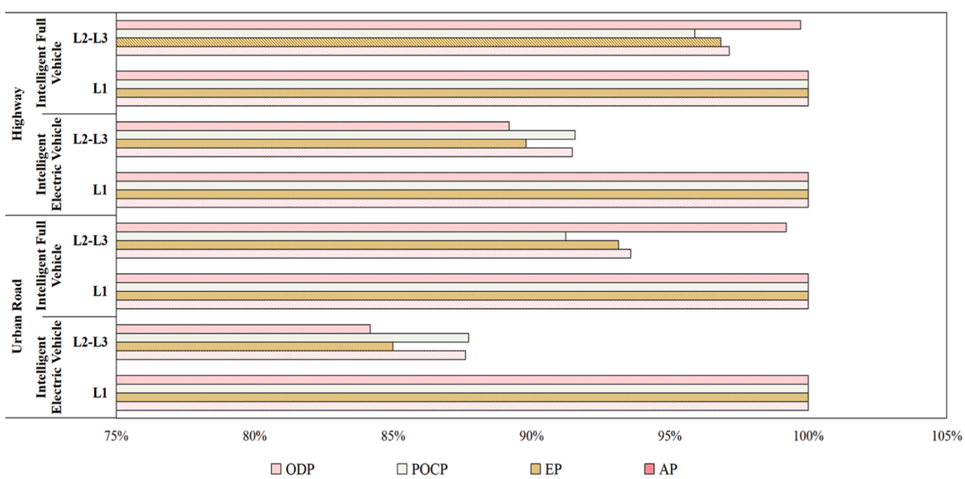

Fig. 6. Change rate of pollutant emission in the whole life cycle of the intelligent coupling multi-operation scenario of two vehicle types.

Fig. 7. Simulation experiment of test site.

positioning. It follows established communication protocols for data exchange, enabling information sharing and interactions between vehicles, vehicles and roads, and vehicles and pedestrians (networked). It covers various levels of automated driving and considers the collaborative optimization between vehicles and roads (system integration). Through system integration, network interconnection, and vehicle automation, a vehicle-road coordinated autonomous driving system was developed. According to the "Energy-Saving and New Energy Vehicle Technology Roadmap 2.0", networked technology is divided into three levels: networked auxiliary information interaction, networked collaborative sensing, and networked collaborative decision-making and control. Networked auxiliary information interaction and networked collaborative sensing are primarily used to assist vehicle intelligence technology, integrating with onboard sensor perception information as input for the vehicle's autonomous driving decision-making and control system to achieve better single vehicle intelligent driving. However, studies have shown that optimizing the control of a single vehicle has limited potential for improving the safety and economy. This section mainly studies collaborative decision-making and control between vehicles and between vehicles and roads, focusing on the impact of multi-intelligent vehicle platooning coordination technology and smart intersections on the life cycle energy consumption and emissions of intelligent electric and fuel vehicles, as shown in Fig. 7.

Considering that numerous factors affect the driving state of automobiles, the aforementioned studies often focused on acceleration, passing time, and other factors under ideal conditions. Therefore, based on field research, it is estimated that intelligent electric vehicles equipped with vehicle-road coordination technology at intersections can achieve energy savings of 15 %-20 %, whereas intelligent fuel vehicles can save 10 %-15 %. Four scenarios were constructed based on two key vehicle-road coordination technologies, considering the operating conditions of intelligent electric vehicles and intelligent fuel vehicles on highways and urban road, as shown in Table 15. The focus was on the impact of changes in electricity and fuel consumption during the operating phase on the overall energy consumption and emissions.

4.2.2. Analysis of vehicle-road coordination results

By applying the constructed scenarios to a previously developed vehicle life cycle assessment model, energy consumption, carbon emissions, and pollutant emissions during the operational phase of intelligent fuel and electric vehicles equipped with vehicle platooning and intersection coordination technologies were obtained for urban and highway scenarios. As in the previous section, only the changes during the operational phase were considered for their impact on the life cycles of the two vehicle types. The life cycle assessment results are presented in Table 16.

The analysis of Fig. 8 indicates that in urban road scenarios, electric vehicles with intersection coordination control reduce their life cycle fossil energy consumption by 8.33 %-10.88 % compared to L2-L3 level single-vehicle intelligent electric vehicles, by 21.71 %-23.89 % compared to L1 level single-vehicle intelligent electric vehicles, and by approximately 58 % compared to fuel vehicles under the same conditions. Fuel vehicles reduce fossil energy consumption by 8.68 %-13.02 % and 15.98 %-19.97 %, respectively. In highway scenarios, electric vehicles with intelligent vehicle platooning coordination control reduce their life cycle fossil energy consumption by 3.70 %-6.18 % compared to L2-L3 level single-vehicle intelligent electric vehicles, by 13.14 %-15.38 % compared to L1 level single-vehicle intelligent electric vehicles, and by approximately 27 % compared to fuel vehicles under the same conditions. Fuel vehicles reduced their fossil energy consumption by 4.65 %-8.19 % and 8.49 %-11.89 %, respectively.

The analysis of Fig. 9 indicates that in urban road scenarios, electric vehicles with intersection coordination control reduce their life cycle carbon emissions by 7.88 %-10.34 % compared to L2-L3 level single-vehicle intelligent electric vehicles, 20.22 %-22.35 % compared to L1 level single-vehicle intelligent electric vehicles, and by approximately 46 % compared to fuel vehicles under the same conditions. Fuel vehicles reduced their carbon emissions by 8.64 %-12.78 % and 15.77 %-19.58 %, respectively. In highway scenarios, electric vehicles with intelligent vehicle platooning coordination control reduce their life cycle carbon emissions by 3.47 %-5.91 % compared to L2-L3 level single-vehicle intelligent electric vehicles, by 12.29 %-14.50 % compared to L1 level single-vehicle intelligent electric vehicles, and by approximately 7.5 % compared to fuel vehicles under the same conditions. Fuel vehicles reduce their carbon emissions by 4.97 %-7.73 % and 8.75 %-11.40 %, respectively.

The analysis of Fig. 10 indicates that in urban road scenarios, electric vehicles with intersection coordination control reduce their life cycle AP, EP, POCP, and ODP by approximately 7 %-12 % compared to L2-L3 level single-vehicle intelligent electric vehicles, and by approximately 14 %-22 % compared to L1 level single-vehicle intelligent electric vehicles. Fuel vehicles, except for ODP, were reduced by approximately 6 %-13 % and 8 %-20 %, respectively. In highway scenarios, electric vehicles with intelligent vehicle platooning coordination control reduce their life cycle AP, EP, POCP, and ODP by approximately 3 %-7 % compared to L2-L3 level single-vehicle intelligent electric vehicles, and by approximately 11 %-17 % compared to L1 level single-vehicle intelligent electric vehicles. Fuel vehicles, except for ODP, were reduced by approximately 3 %-9 % and 6 %-12 %, respectively.

In summary, vehicles equipped with vehicle-road coordination technology can further reduce their life cycle fossil energy consumption, carbon emissions, and pollutant emissions beyond the capabilities of single-vehicle intelligence. Thus, the implementation of intelligent and networked technology is crucial for reducing the life cycle energy consumption and vehicle emissions.

4.3. Scenario simulation study on intelligent vehicle electrification considering regional differences

4.3.1. Setting regional differences scenarios

As of September 2023, 17 national-level intelligent networked demonstration zones have been established, located in areas under six divisions of the State Grid and the Southern Power Grid. The power structures in these regions vary, and this section focuses on the impact of

Table 15
Four kinds of vehicle-road cooperative coupling multi-operation scenarios(Zheng et al., 2015; Alrifaee et al., 2015; Amini et al., 2019; Wei et al., 2019; Wang and Guo, 2019; Zhang et al., 2019; Liao et al., 2022).

Scenario	Vehicle Type	Vehicle-to-Infrastructure Technology	Operating Scenario	Energy Efficiency Rate	Energy Consumption/Fuel Consumption per 100 Kilometers
Scenario 1	Intelligent Electric Vehicle	Platooning Cooperative Control	Urban Road	6 %–10 %	15.3 ~ 15.98/ kWh·100 km^{-1}
Scenario 2		Intersection Cooperative Control	Highway	15 %–20 %	10.4 ~ 11.05 kWh·100 km^{-1}
Scenario 1	Intelligent Fuel Vehicle	Platooning Cooperative Control	Urban Road	6 %–10 %	6.03 ~ 6.3 L·100 km^{-1}
Scenario 2		Intersection Cooperative Control	Highway	10 %–15 %	9.1 ~ 9.63 L·100 km^{-1}

Table 16
Full life cycle evaluation results of vehicle-road collaborative coupling multi-operation scenarios for two models.

Scenario	ADP(f)/MJ	GWP/kg	AP/kg	EP/kg	POCP/kg	ODP/kg
Scenario 1	3.02E+ 05 ~ 3.10E+ 05	3.09E+ 04 ~ 3.17E+ 04	7.11E+ 01 ~ 7.27E+ 01	7.92E+ 00 ~ 8.14E+ 00	4.64E+ 00 ~ 4.74E+ 00	2.77E−07 ~ 2.85E−07
Scenario 2	2.45E+ 05 ~ 2.52E+ 05	2.55E+ 04 ~ 2.62E+ 04	5.97E+ 01 ~ 6.12E+ 01	6.36E+ 00 ~ 6.57E+ 00	3.91E+ 00 ~ 4.00E+ 00	2.19E−07 ~ 2.27E−07
Scenario 1	4.15E+ 05 ~ 4.31E+ 05	3.34E+ 04 ~ 3.44E+ 04	4.18E+ 01 ~ 4.28E+ 01	5.45E+ 00 ~ 5.61E+ 00	1.06E+ 01 ~ 1.11E+ 01	6.11E−08 ~ 6.12E−08
Scenario 2	5.81E+ 05 ~ 6.10E+ 05	4.64E+ 04 ~ 4.86E+ 04	5.37E+ 01 ~ 5.58E+ 01	7.14E+ 00 ~ 7.43E+ 00	1.53E+ 01 ~ 1.61E+ 01	6.26E−08 ~ 6.29E−08

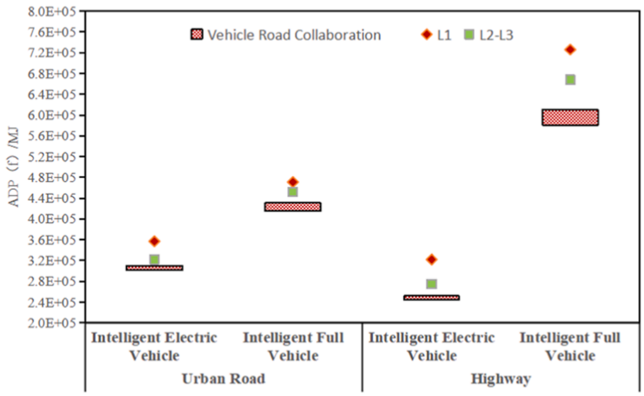

Fig. 8. Full life cycle of vehicle-road collaborative coupling multi-operation scenario of two models ADP(f).

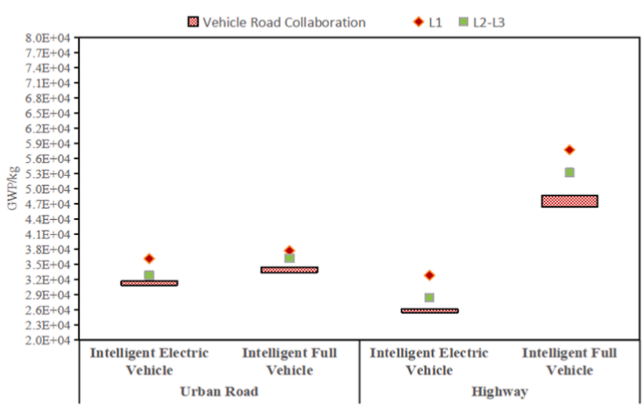

Fig. 9. Full life cycle of vehicle-road collaborative coupling multi-operation scenario of two models GWP.

regional power structure differences on the life cycle energy consumption and environmental emissions of intelligent electric vehicles. The manufacturing and operational phases of intelligent electric vehicles generate large amounts of carbon dioxide and pollutants primarily because of the significant electricity consumption during these phases. The carbon and pollutant emission intensities of this electricity depend on its power structure. The carbon emission intensity of traditional energy generation technologies (coal, oil, and natural gas) is several to dozens of times higher than that of renewable energy generation technologies (solar and wind). For example, with a consumption rate of 18 kWh per 100 km, the Tesla Model S emits 107.6 g of carbon per kilometer in China, compared to 70 g in the USA and 63 g in Germany. Therefore, differences in power structures significantly affect energy consumption and environmental emissions during the raw material acquisition, manufacturing, and operational phases of intelligent electric vehicles. Furthermore, in 2023, the National Development and Reform Commission and other departments issued "Implementation Opinions on Strengthening the Integration and Interaction of New Energy Vehicles with the Power Grid," emphasizing the flexible adjustment capability of new energy vehicle power batteries as controllable loads or mobile storage to support the efficient and economic operation of the new power system. Electric vehicles, with their mobile storage and controllable load characteristics, can utilize V2G technology to provide grid-friendly loads and mobile distributed power sources. They can provide services such as peak shaving, valley filling, and frequency regulation, ensuring power balance and improving the overall operational efficiency of the power system.

In summary, studying the life cycle energy consumption and environmental emissions of intelligent electric vehicles under different power structures across various regions in China will help optimize the layout of the intelligent electric vehicle industry, increase the penetration rate of intelligent electric vehicles, and foster a new industrial ecosystem for vehicle-grid integration. An analysis of the 2023 regional power generation and power structure data from the National Bureau of Statistics reveals the power structure scenarios of different regions in China, as shown in Table 17. Among them, the North China region had the highest proportion of thermal power generation, whereas the Southwest region had the lowest. In terms of renewable energy generation, the Southwest and South China regions have a higher proportion of hydropower, whereas the Northeast and Northwest regions have a higher proportion of wind power.

The emission coefficients of the power grid utilized in this academic study are characterized by their average nature, regional specificity, and static quality. In the quantitative analysis conducted, particular emphasis was placed on the careful selection and utilization of these grid emission coefficients. These coefficients are designed to encompass three critical aspects: the average emission levels, regional peculiarities, and the historical consistency of emissions. This approach ensures that the analytical framework is both comprehensive and precise.

The coefficients encompass not only the national average emission levels but also take into account the distinct power grid configurations across the six major regions: East China, Central China, North China, Northwest, Northeast, and South China. Additionally, they provide a stable historical reference for emission coefficients, thereby circumventing the complexities that could arise from dynamic temporal adjustments.The resultant data model not only strengthens the research's foundation but also enhances the precision of environmental impact assessments for smart electric vehicles. This, in turn, offers robust data support for subsequent policy analysis and technological refinement.

4.3.2. Analysis of results considering regional differences

Based on the life cycle assessment results of intelligent electric vehicles under China's average power structure, an in-depth study was conducted on the impact of power structure differences in seven major regions of China, including North China, Central China, and South China, on the life cycle energy consumption and environmental emissions of intelligent electric vehicles. The life cycle assessment results for intelligent electric vehicles under power structure differences in these seven major regions are listed in Table 18.

As shown in Table 18, the life cycle energy consumption, carbon emissions, and pollutant emissions of intelligent electric vehicles based on the power structure in North China, except for ODP, were the highest. This is mainly because the proportion of thermal power generation is the highest in this region, and the combustion of fossil fuels generates large amounts of CO2 and pollutants. The life cycle ADP(f), GWP, AP, EP, ODP, and POCP values were 3.45E+ 05 MJ, 3.50E+ 04 kg, 7.96E+ 01 kg, 9.09E+ 00 kg, 1.38E-07 kg, and 5.18E+ 00 kg,

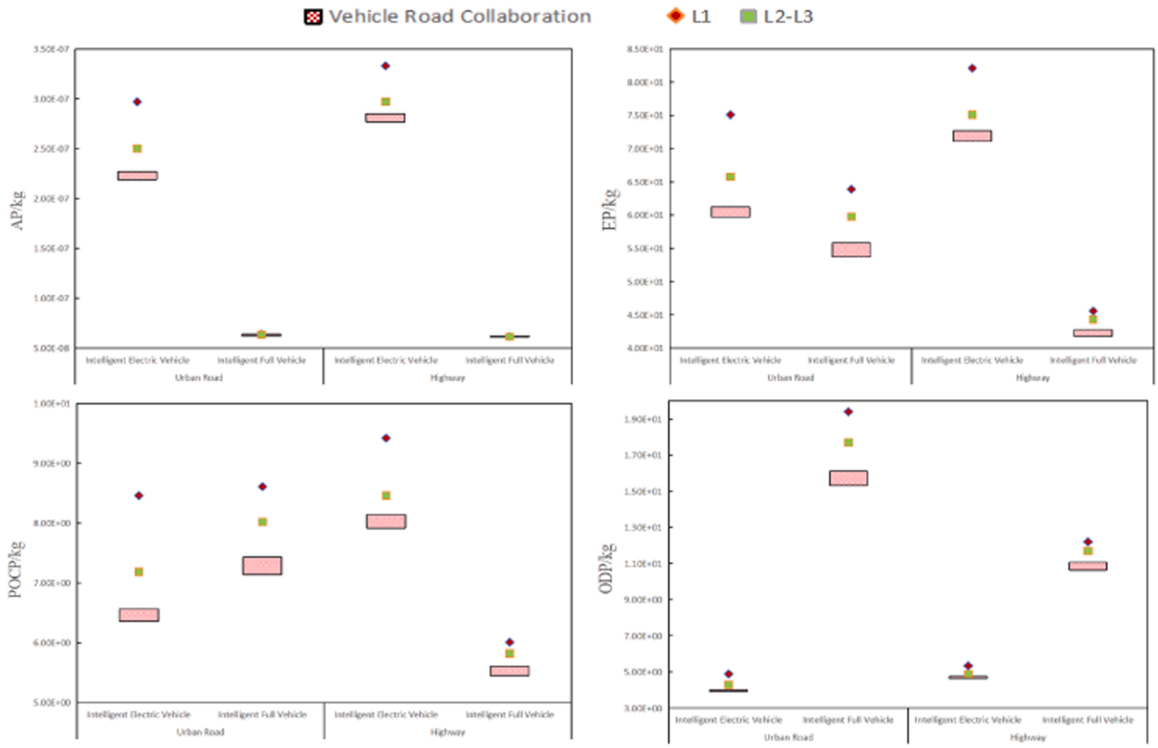

Fig. 10. Pollutant emission in the whole life cycle of the multi-operation scenario of vehicle-road collaborative coupling of two models.

Table 17
Power structure in different regions of China.

Region	Thermal Power	Hydroelectric Power	Nuclear Power	Wind Power	Solar Power
North China	85.1 %	0.8 %	1.3 %	10.4 %	2.4 %
Central China	69.9 %	18.7 %	0.0 %	8.4 %	3.0 %
South China	57.3 %	24.5 %	10.6 %	5.2 %	2.4 %
East China	77.9 %	2.7 %	11.8 %	5.5 %	2.1 %
Northeast China	74.5 %	1.6 %	4.2 %	16.8 %	2.9 %
Northwest China	71.8 %	8.6 %	0.0 %	12.3 %	7.3 %
Southwest China	29.9 %	65.7 %	0.0 %	3.5 %	0.9 %

respectively. The Southwest region, benefiting from its abundant hydropower resources, has the lowest life-cycle energy consumption, carbon emissions, and pollutant emissions. Its life cycle ADP(f), GWP, AP, EP, ODP, and POCP were 1.52E+ 05 MJ, 1.68E+ 04 kg, 4.11E+ 01 kg, 3.84E+ 00 kg, 6.28E-08 kg, and 2.73E+ 00 kg, respectively. Compared with the North China region, the Southwest region's energy consumption, carbon emissions, and pollutant emissions decreased by 55.94 %, 52.00 %, 48.37 %, 57.76 %, 54.49 %, and 47.30 %, respectively. This proves that reducing the proportion of thermal power generation and increasing the proportion of renewable energy generation helps to reduce the life cycle energy consumption, carbon emissions, and pollutant emissions of intelligent electric vehicles. Additionally, the life cycle assessment results of intelligent electric vehicles based on the power structures in the Northeast, Northwest, and East China regions were similar, except for the ODP. The Northwest region has the highest ODP emissions in the country, mainly because of the high proportion of solar power generation in its power structure.

Regarding fossil energy consumption, Fig. 11 illustrates the life cycle fossil energy consumption of intelligent electric vehicles across the different power structures of seven major regions. The analysis of Fig. 11 reveals that the life cycle fossil energy consumption of intelligent electric vehicles based on the power structure of North China is the highest. Compared to the national power structure, fossil energy consumption during the raw material acquisition stage was roughly equal, whereas it increased by 23.02 % and 26.54 % during the manufacturing, assembly, and operation stages, respectively, and decreased by 14.49 % in the scrapping and recycling stages, resulting in an overall life cycle increase of 22.78 %. Compared to the national average, the life cycle fossil energy consumption ADP(f) increased by 3.91 %, 13.88 %, 9.61 %, and 6.41 % in Central, East, Northeast, and Northwest China, respectively, and decreased by 11.74 % and 45.91 % in South and Southwest China, respectively.

Regarding carbon emissions, Fig. 12 illustrates the life cycle carbon emissions of intelligent electric vehicles across different power structures of the seven major regions. The analysis of Fig. 12 reveals that the life cycle fossil energy consumption of intelligent electric vehicles based on the power structure of Southwest China is the lowest. Compared to the national power structure, fossil energy consumption during the manufacturing, assembly, and operation stages decreased by 45.58 % and 54.04 %, respectively. Carbon emissions during the operation stage were significantly lower than those in North and East China, amounting to 36.15 % and 39.43 % of the total emissions in these two regions, respectively. However, carbon emissions during the scrapping and recycling stage increase by 27.76 %, resulting in an overall life cycle reduction of 41.87 %. The life cycle carbon emissions GWP increased by 21.11 %, 3.81 %, 13.15 %, 9.34 %, and 6.23 % in North China, Central China, East China, Northeast China, and Northwest China, respectively, whereas it decreased by 10.38 % in South China.

In addition, because intelligent fuel vehicles do not consume electricity during their operation, differences in power structures have no significant impact on their carbon emissions during this stage. To better compare the potential of intelligent electric vehicles and intelligent fuel vehicles in reducing carbon emissions under different regional power structures, the carbon emission differences during the operation stage of intelligent electric vehicles and intelligent fuel vehicles in various regions were specifically studied, as shown in Fig. 13. Compared to

Table 18
Full life cycle evaluation results of intelligent electric vehicles under power structure difference scenario.

Region	Stage	ADP(e)/kg	ADP(f)/MJ	GWP/kg	AP/kg	EP/kg	POCP/kg
North China	I	9.88E+ 04	1.21E+ 04	4.91E+ 01	2.47E+ 00	2.09E−08	3.91E+ 00
	II	7.75E+ 04	7.36E+ 03	1.55E+ 01	2.11E+ 00	2.70E−08	9.85E−01
	III	2.05E+ 05	1.92E+ 04	4.03E+ 01	5.52E+ 00	8.10E−08	2.59E+ 00
	IV	−3.66E+ 04	−3.66E+ 03	−2.53E+ 01	−1.02E+ 00	8.68E−09	−2.31E+ 00
	Total	3.45E+ 05	3.50E+ 04	7.96E+ 01	9.09E+ 00	1.38E−07	5.18E+ 00
Central China	I	9.87E+ 04	1.21E+ 04	4.91E+ 01	2.47E+ 00	2.10E−08	3.91E+ 00
	II	6.55E+ 04	6.24E+ 03	1.31E+ 01	1.78E+ 00	3.36E−08	8.33E−01
	III	1.69E+ 05	1.58E+ 04	3.32E+ 01	4.55E+ 00	1.01E−07	2.14E+ 00
	IV	−4.17E+ 04	−4.14E+ 03	−2.63E+ 01	−1.16E+ 00	1.15E−08	−2.37E+ 00
	Total	2.92E+ 05	3.00E+ 04	6.90E+ 01	7.64E+ 00	1.67E−07	4.51E+ 00
South China	I	9.86E+ 04	1.21E+ 04	4.90E+ 01	2.46E+ 00	2.09E−08	3.90E+ 00
	II	5.57E+ 04	5.30E+ 03	1.11E+ 01	1.52E+ 00	8.08E−08	7.09E−01
	III	1.40E+ 05	1.30E+ 04	2.73E+ 01	3.75E+ 00	2.69E−08	1.77E+ 00
	IV	−4.60E+ 04	−4.55E+ 03	−2.72E+ 01	−1.27E+ 00	8.65E−09	−2.43E+ 00
	Total	2.48E+ 05	2.59E+ 04	6.03E+ 01	6.46E+ 00	1.37E−07	3.95E+ 00
East China	I	9.88E+ 04	1.21E+ 04	4.91E+ 01	2.47E+ 00	2.08E−08	3.91E+ 00
	II	7.18E+ 04	6.83E+ 03	1.43E+ 01	1.96E+ 00	7.10E−08	9.14E−01
	III	1.88E+ 05	1.76E+ 04	3.70E+ 01	5.07E+ 00	2.36E−08	2.38E+ 00
	IV	−3.90E+ 04	−3.89E+ 03	−2.58E+ 01	−1.08E+ 00	7.24E−09	−2.34E+ 00
	Total	3.20E+ 05	3.27E+ 04	7.46E+ 01	8.41E+ 00	1.23E−07	4.86E+ 00
Northeast China	I	9.87E+ 04	1.21E+ 04	4.91E+ 01	2.47E+ 00	2.10E−08	3.91E+ 00
	II	6.92E+ 04	6.58E+ 03	1.38E+ 01	1.89E+ 00	9.76E−08	8.80E−01
	III	1.80E+ 05	1.69E+ 04	3.54E+ 01	4.85E+ 00	3.25E−08	2.28E+ 00
	IV	−4.01E+ 04	−4.00E+ 03	−2.60E+ 01	−1.11E+ 00	1.11E−08	−2.35E+ 00
	Total	3.08E+ 05	3.16E+ 04	7.23E+ 01	8.09E+ 00	1.62E−07	4.71E+ 00
Northwest China	I	9.87E+ 04	1.21E+ 04	4.91E+ 01	2.47E+ 00	2.16E−08	3.91E+ 00
	II	6.72E+ 04	6.39E+ 03	1.34E+ 01	1.83E+ 00	2.44E−07	8.56E−01
	III	1.74E+ 05	1.63E+ 04	3.42E+ 01	4.68E+ 00	8.14E−08	2.21E+ 00
	IV	−4.10E+ 04	−4.08E+ 03	−2.62E+ 01	−1.14E+ 00	3.22E−08	−2.36E+ 00
	Total	2.99E+ 05	3.07E+ 04	7.05E+ 01	7.84E+ 00	3.79E−07	4.61E+ 00
Southwest China	I	9.83E+ 04	1.21E+ 04	4.90E+ 01	2.46E+ 00	2.07E−08	3.90E+ 00
	II	3.40E+ 04	3.26E+ 03	6.80E+ 00	9.27E−01	3.06E−08	4.33E−01
	III	7.51E+ 04	6.94E+ 03	1.44E+ 01	1.98E+ 00	1.02E−08	9.42E−01
	IV	−5.53E+ 04	−5.43E+ 03	−2.90E+ 01	−1.53E+ 00	1.42E−09	−2.55E+ 00
	Total	1.52E+ 05	1.68E+ 04	4.11E+ 01	3.84E+ 00	6.28E−08	2.73E+ 00

Note: I represents the Raw Material Acquisition stage, II represents the Manufacturing and Assembly stage, III represents the Operation and Use stage, IV represents the End-of-Life Recycling stage, and the Total represents Life Cycle Assessment.

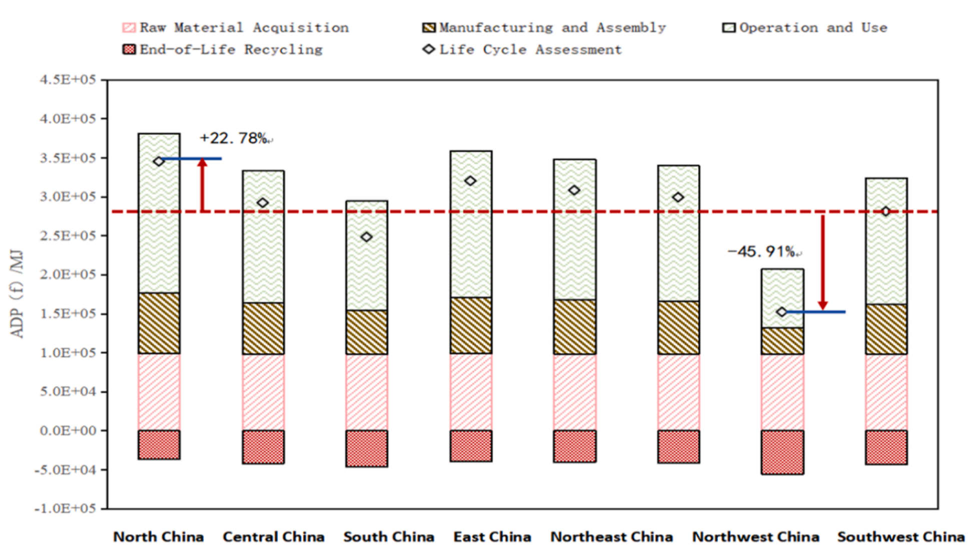

Fig. 11. Fossil energy consumption in the whole life cycle of intelligent electric vehicles under the power structure difference scenario.

intelligent fuel vehicles, carbon emissions during the operation stage of intelligent electric vehicles in North, Central, South, East, Northeast, Northwest, and Southwest China decreased by 37.25 %, 48.37 %, 57.52 %, 42.48 %, 44.77 %, 46.73 %, and 77.32 %, respectively.

Regarding pollutant emissions, using the national power structure scenario as a baseline, changes in the life cycle pollutant emissions of intelligent electric vehicles under different regional power structures are shown in Fig. 14. The analysis of Fig. 14 reveals that, regionally, intelligent electric vehicles based on the power structure of Southwest China have the lowest life cycle pollutant emissions. The AP, EP, ODP, and POCP were only 61.43 %, 52.24 %, 24.53 %, and 62.47 % of the national power structure baseline and 51.63 %, 42.24 %, 45.51 %, and 52.70 % of the North China power structure baseline, respectively. From the perspective of pollutant types, considering the national power

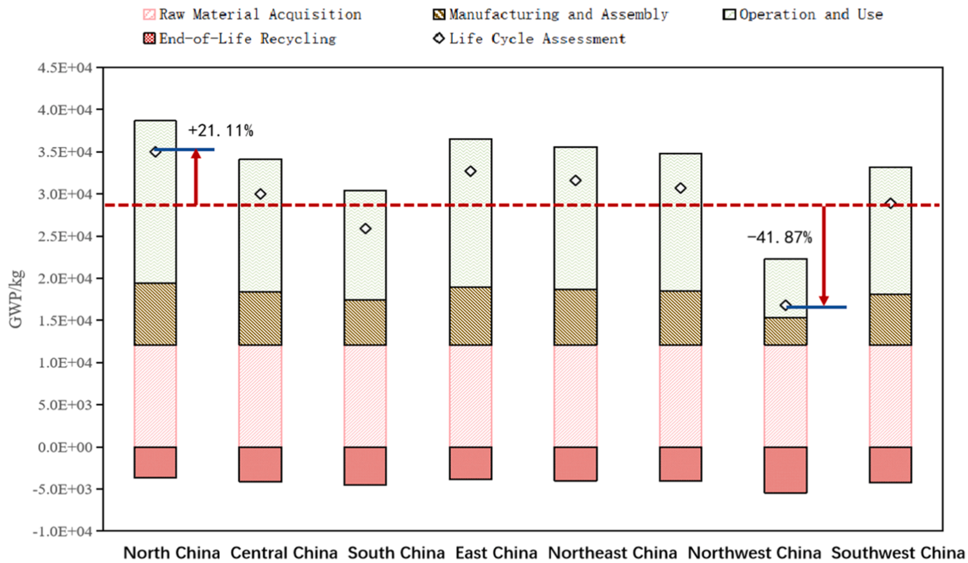

Fig. 12. Life cycle carbon emissions of intelligent electric vehicles under power structure difference scenario.

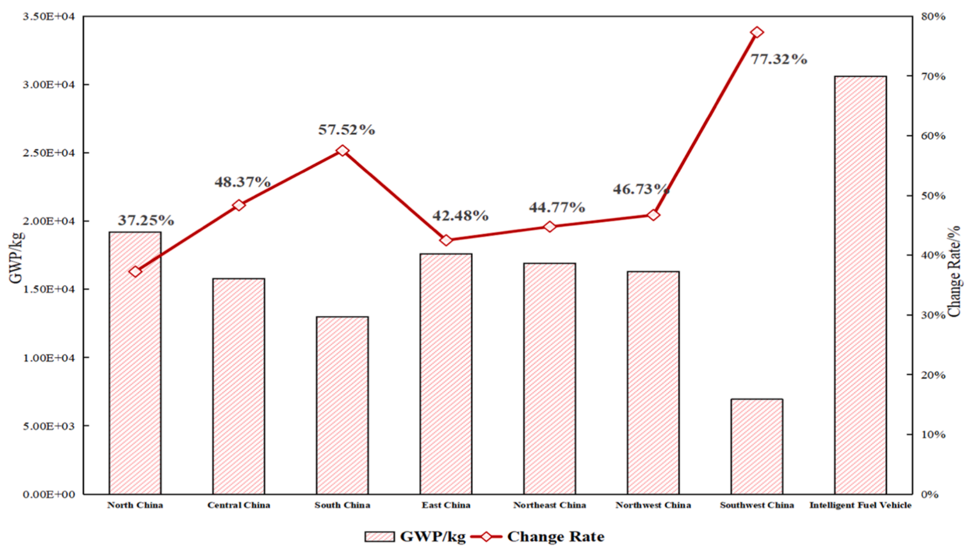

Fig. 13. Carbon emissions during operation and use under the power structure difference scenario of intelligent electric vehicles and intelligent fuel vehicles.

structure as a baseline, the life cycle AP of intelligent electric vehicles increased by 18.98 %, 3.14 %, 11.51 %, 8.07 %, and 5.38 % in North China, Central China, East China, Northeast China, and Northwest China, respectively, and decreased by 9.87 % and 38.57 % in South China and Southwest China, respectively. The life cycle EP of intelligent electric vehicles increased by 23.67 %, 3.95 %, 14.42 %, 10.07 %, and 6.67 % in North, Central, East, Northeast, and Northwest China, respectively, whereas it decreased by 12.11 % and 47.76 % in South and Southwest China, respectively. The life cycle ODP of intelligent electric vehicles decreased by 46.09 %, 34.77 %, 46.48 %, 51.95 %, 36.72 %, and 75.47 % in North China, Central China, South China, East China, Northeast China, and Southwest China, respectively, and increased by 48.05 % in Northwest China. The life cycle POCP of intelligent electric vehicles increased by 18.54 %, 3.20 %, 11.21 %, 7.78 %, and 5.49 % in North, Central, East, Northeast, and Northwest China, respectively, whereas it decreased by 9.61 % and 37.53 % in South and Southwest China, respectively.

In summary, the higher the proportion of renewable energy in the power structure and the lower the proportion of thermal power, the lower the life cycle ADP(f), GWP, AP, EP, and POCP of intelligent electric vehicles. Overall, the fossil energy consumption and environmental emissions of intelligent electric vehicles in the eastern and southern regions of China were lower than those in the northern and western regions. This aligns with the currently higher penetration rates of new energy vehicles in South and East China than in North and West China. This demonstrates that a higher proportion of clean energy in the power structure is conducive to increasing the penetration rate of new energy vehicles while reducing carbon and pollutant emissions.

5. Predictions

5.1. Scenario construction for 2035

Based on the life cycle assessment results from this study and scenario simulation studies that focused on key factors, the critical factors affecting the life cycle energy consumption and vehicle emissions were identified. Key factors such as vehicle lightweight coefficients, fuel/electricity consumption per 100 kilometers, and power structure were comprehensively selected to scientifically predict the life cycle assessment results of intelligent electric vehicles and intelligent fuel vehicles

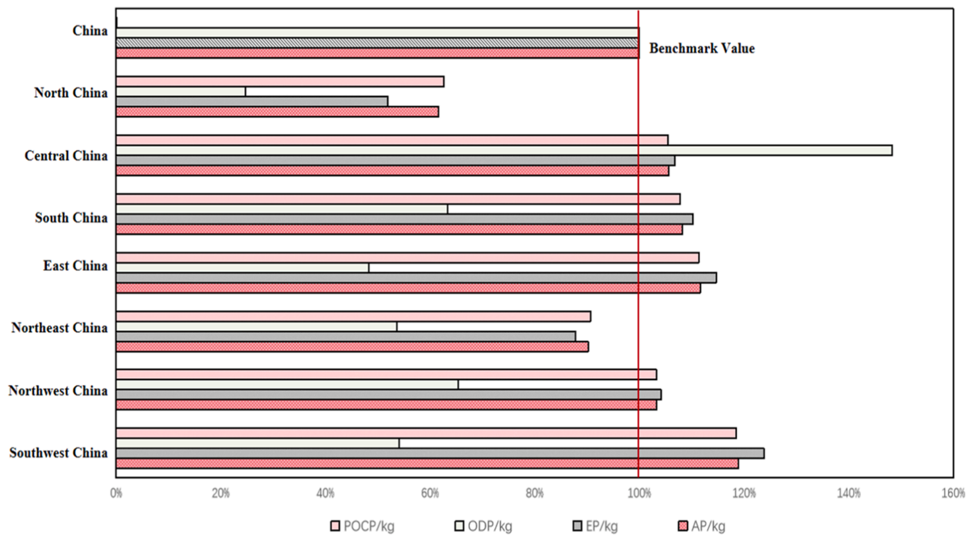

Fig. 14. The change of pollutant emissions in the whole life cycle of intelligent electric vehicles under the power structure difference scenario.

for the years 2025, 2030, and 2035 by integrating the prospects and requirements for pure electric vehicles, traditional fuel vehicles, and intelligent connected vehicles as outlined in the "Energy-Saving and New Energy Vehicle Technology Roadmap 2.0".(The Chinese Society of Automotive Engineering, 2020)

According to the technology roadmap for pure electric and traditional energy vehicles, the energy consumption of a typical A-class BEV with leading technology is projected to be less than 11 kWh/100 km by 2025, less than 10.5 kWh/100 km by 2030, and less than 10 kWh/100 km by 2035. For traditional energy passenger cars, fuel consumption is projected to be 5.6 L/100 km (WLTC) by 2025, 4.8 L/100 km (WLTC) by 2030, and 4 L/100 km (WLTC) by 2035. According to the lightweight technology roadmap, the lightweight coefficients for traditional energy vehicles are expected to decrease by 10 %, 18 %, and 25 % by 2025, 2030, and 2035, respectively, whereas those for electric vehicles are expected to decrease by 15 %, 25 %, and 35 %, respectively. According to the intelligent connected vehicle technology roadmap, vehicles with integrated vehicle-road-cloud collaborative decision-making and control functions are expected to enter the market by 2030. HA-level intelligent connected vehicles are expected to be widely used on highways and on a large scale on certain urban road. By 2035, China aims to have a more complete intelligent connected vehicle industry system, deeply integrated with intelligent transportation and smart city ecosystems, with various types of connected, highly automated driving vehicles operating widely across the country. Considering the potential for energy savings and emission reduction from single-vehicle intelligence and vehicle-road collaboration, it is assumed that the operational efficiency of intelligent vehicles will improve by 10 % by 2025, 15 % by 2030, and 30 % by 2035. The predicted scenarios are listed in Table 19.

At present, there are three main paths for automotive lightweighting: structural optimization to make components thinner, hollow, smaller, or composite; The use of new materials, such as high-strength steel, aluminum, and non-metallic materials; Process improvement mainly includes forming and connecting technologies, as shown in Table 20

Table 19
Intelligent vehicle forecast scenarios for 2035.

Parameter		2023	2025	2030	2035
Intelligent Electric Vehicle	Energy Consumption per 100 Kilometers/ kg·100 km^{-1}	13.5	11	10.5	10
	Lightweight Index/%	-	15 %	25 %	35 %
	Energy Density/ Wh·kg^{-1}	150	225	250	275
Intelligent Fuel Vehicle	Energy Consumption per 100 Kilometers/ kg·100 km^{-1}	7.18	5.6	4.8	4
	Lightweight Index/%	-	10 %	18 %	25 %
Percentage Improvement in Intelligent Connectivity Performance/%		-	10 %	15 %	30 %
Electrical Structure	Proportion of Thermal Power	66.6 %	59.6 %	52.3 %	40 %
	Proportion of Hydroelectric Power	15.3 %	15.8 %	16.1 %	17 %
	Proportion of Nuclear Power	4.7 %	6.8 %	7.5 %	9 %
	Proportion of Wind Power	8.6 %	10.9 %	14.3 %	19 %
	Proportion of Solar Power	4.8 %	6.9 %	9.8 %	15 %

Note: The power structure in 2030 and 2035 comprehensively refer to the report "China's 2030 Energy and Power Development Planning Research and 2060 Outlook", and combined with the forecast analysis of power demand and power structure of many professional institutions in the power industry.

5.2. Analysis of predictions for 2035

5.2.1. Prediction results

Based on the relevant data from the scenario construction for 2035 and using the vehicle life cycle assessment model established earlier, the ADP(e), ADP(f), GWP, AP, EP, POCP, and ODP results for the life cycles of intelligent electric vehicles and intelligent fuel vehicles for the years 2025, 2030, and 2035 were obtained, as shown in Table 21. Data analysis indicates that from 2025 to 2035, the life cycle consumption of mineral resources, fossil energy, carbon emissions, and pollutant emissions for both intelligent electric vehicles and intelligent fuel vehicles will be significantly reduced compared to 2023. The most notable decreases were observed in fossil energy consumption, carbon emissions, and acidification potential AP, with intelligent electric vehicles showing a more pronounced reduction than intelligent fuel vehicles. This strongly demonstrates that with the advancement of vehicle lightweighting technology, reduction in energy consumption per 100 km, and increase in battery energy density, the potential for energy saving and emission reduction in intelligent electric vehicles is further enhanced.

5.2.2. Results analysis

Based on the prediction results, this section analyzes the resource

Table 20
Automotive Lightweight Technology Route.

Technical type	Detailed Classification			
Lightweight Technology for Vehicles	Lightweight Materials	High strength steel: SAPH440 DP980 、CP780 、TWIP780、 Hot stamping steel, 20NiCrMo7, etc. Aluminum alloy: aluminum alloy sheet, cast aluminum alloy, forged aluminum alloy, etc. Magnesium alloys: magnesium alloy sheets, cast magnesium alloys, forged magnesium alloys, etc. Non metallic materials: glass fiber/carbon fiber/basalt fiber and other reinforced composite materials, high-performance cash engineering materials, vehicle structure reinforcement adhesives, etc.		
	Advanced Technology	Manufacturing Process	Automotive Steel (Plate)	Hydraulic forming (internal high-pressure forming), hot stamping forming, roll forming, laser welding, uneven thickness rolled plates, etc.
			Magnesium alloy/ aluminum alloy.	Semi solid forming, high-pressure casting forming, low (poor) die casting forming, etc.
			Composite	Online molding, online injection molding, online compression molding, etc.
		Connection Process		Laser welding and laser brazing, friction stir welding, locking riveting and self-locking riveting technology, hot melt self tapping screws, adhesive connections, etc.
	Structural Optimization	Topology optimization of vehicle and component structure, size optimization of vehicle and component. Optimization of vehicle and component shape/morphology. Multidisciplinary/multi-objective optimization of the entire vehicle, its components, and assemblies.		

Table 21
Full life cycle evaluation results of intelligent electric vehicles and intelligent fuel vehicles for 2035.

Vehicle Type	Year	Stage	ADP(e)/kg	ADP(f)/MJ	GWP/kg	AP/kg	EP/kg	POCP/kg	ODP/kg
Intelligent Electric Vehicle	2025	I	3.34E−01	7.77E+ 04	9.08E+ 03	3.67E+ 01	1.92E+ 00	1.51E−08	3.02E+ 00
		II	7.57E−04	4.59E+ 04	4.36E+ 03	9.18E+ 00	1.25E+ 00	6.19E−08	5.86E−01
		III	2.08E−03	1.08E+ 05	9.99E+ 03	2.10E+ 01	2.87E+ 00	1.69E−07	1.36E+ 00
		IV	−2.72E−01	−3.59E+ 04	−3.53E+ 03	−2.06E+ 01	−9.78E−01	2.25E−08	−1.89E+ 00
		Total	6.42E−02	1.95E+ 05	1.99E+ 04	4.62E+ 01	5.07E+ 00	2.69E−07	3.08E+ 00
	2030	I	2.98E−01	6.90E+ 04	8.09E+ 03	3.27E+ 01	1.70E+ 00	1.39E−08	2.68E+ 00
		II	9.17E−04	3.67E+ 04	3.49E+ 03	7.35E+ 00	1.00E+ 00	7.78E−08	4.69E−01
		III	2.56E−03	8.61E+ 04	7.95E+ 03	1.67E+ 01	2.29E+ 00	2.16E−07	1.09E+ 00
		IV	−2.43E−01	−3.35E+ 04	−3.29E+ 03	−1.87E+ 01	−9.13E−01	2.93E−08	−1.70E+ 00
		Total	5.85E−02	1.58E+ 05	1.62E+ 04	3.81E+ 01	4.08E+ 00	3.37E−07	2.54E+ 00
	2035	I	2.63E−01	6.02E+ 04	7.13E+ 03	2.89E+ 01	1.49E+ 00	1.27E−08	2.35E+ 00
		II	1.17E−03	2.62E+ 04	2.50E+ 03	5.28E+ 00	7.17E−01	1.04E−07	3.38E−01
		III	2.93E−03	5.35E+ 04	4.86E+ 03	1.02E+ 01	1.40E+ 00	2.59E−07	6.77E−01
		IV	−2.16E−01	−3.18E+ 04	−3.12E+ 03	−1.70E+ 01	−8.70E−01	4.08E−08	−1.53E+ 00
		Total	5.15E−02	1.08E+ 05	1.14E+ 04	2.74E+ 01	2.74E+ 00	4.17E−07	1.84E+ 00
Intelligent Fuel Vehicle	2025	I	1.11E−01	6.63E+ 04	6.07E+ 03	2.25E+ 01	1.55E+ 00	4.18E−09	2.36E+ 00
		II	7.20E−04	4.15E+ 04	3.95E+ 03	8.31E+ 00	1.13E+ 00	5.90E−08	5.30E−01
		III	1.31E−03	2.77E+ 05	2.15E+ 04	1.98E+ 01	2.82E+ 00	2.79E−09	7.72E+ 00
		IV	−7.46E−02	−3.73E+ 04	−3.64E+ 03	−1.56E+ 01	−9.58E−01	1.08E−08	−1.68E+ 00
		Total	3.86E−02	3.48E+ 05	2.79E+ 04	3.50E+ 01	4.55E+ 00	7.67E−08	8.92E+ 00
	2030	I	1.01E−01	6.03E+ 04	5.52E+ 03	2.04E+ 01	1.41E+ 00	4.47E−09	2.15E+ 00
		II	8.97E−04	3.39E+ 04	3.22E+ 03	6.79E+ 00	9.25E−01	7.62E−08	4.34E−01
		III	1.07E−03	2.25E+ 05	1.75E+ 04	1.61E+ 01	2.30E+ 00	2.32E−09	6.26E+ 00
		IV	−6.79E−02	−3.48E+ 04	−3.40E+ 03	−1.44E+ 01	−8.95E−01	1.44E−08	−1.54E+ 00
		Total	3.51E−02	2.84E+ 05	2.28E+ 04	2.89E+ 01	3.74E+ 00	9.74E−08	7.30E+ 00
	2035	I	9.26E−02	5.49E+ 04	5.03E+ 03	1.87E+ 01	1.29E+ 00	5.17E−09	1.96E+ 00
		II	1.20E−03	2.49E+ 04	2.37E+ 03	5.02E+ 00	6.81E−01	1.07E−07	3.21E−01
		III	7.40E−04	1.56E+ 05	1.20E+ 04	1.11E+ 01	1.59E+ 00	1.69E−09	4.31E+ 00
		IV	−6.20E−02	−3.30E+ 04	−3.22E+ 03	−1.34E+ 01	−8.51E−01	2.06E−08	−1.43E+ 00
		Total	3.25E−02	2.03E+ 05	1.62E+ 04	2.14E+ 01	2.71E+ 00	1.34E−07	5.16E+ 00

Note: I represents the Raw Material Acquisition stage, II represents the Manufacturing and Assembly stage, III represents the Operation and Use stage, IV represents the End-of-Life Recycling stage, and the Total represents Life Cycle Assessment.

consumption, carbon emissions, and pollutant emissions of intelligent electric vehicles and intelligent fuel vehicles for the years 2025, 2030, and 2035. It also provides a comparative analysis of the energy-saving and emission reduction performance of intelligent electric vehicles versus intelligent fuel vehicles.

5.2.2.1. Mineral resource consumption. The life cycle ADP(e) for intelligent electric vehicles in 2025, 2030, and 2035 were 6.42E-02, 5.85E-02, and 5.15E-02 kg, respectively, representing reductions of 27.7 %, 34.15 %, and 42.00 %, respectively, compared to 2023. For intelligent fuel vehicles, the life cycle ADP(e) in 2025, 2030, and 2035 were 3.86E-02 kg, 3.51E-02 kg, and 2.67E-02 kg, respectively, representing reductions of 10.44 %, 18.64 %, and 24.59 %, respectively, compared with 2023. The life cycle mineral resource consumption ADP(e) for intelligent electric vehicles and intelligent fuel vehicles towards 2035 is shown in Fig. 15.

In 2025, 2030, and 2035, the life cycle mineral resource consumption of intelligent electric vehicles is approximately 1.6 times that of intelligent fuel vehicles. To explore the key factors affecting the ADP(e) of mineral resource consumption for intelligent electric vehicles and intelligent fuel vehicles, the ADP(e) during the raw material acquisition stage for the components of these vehicles was analyzed, as shown in Fig. 15. The analysis of Fig. 16 indicates that the primary reason for the reduction in mineral resource consumption for intelligent electric vehicles is the significant increase in battery energy density, which greatly reduces mineral resource consumption during the raw material acquisition stage. Compared to 2023, mineral resource consumption during the raw material acquisition stage for power batteries is expected to decrease by 33.3 %, 40 %, and 45.61 % in 2025, 2030, and 2035, respectively. Therefore, to further reduce the mineral resource

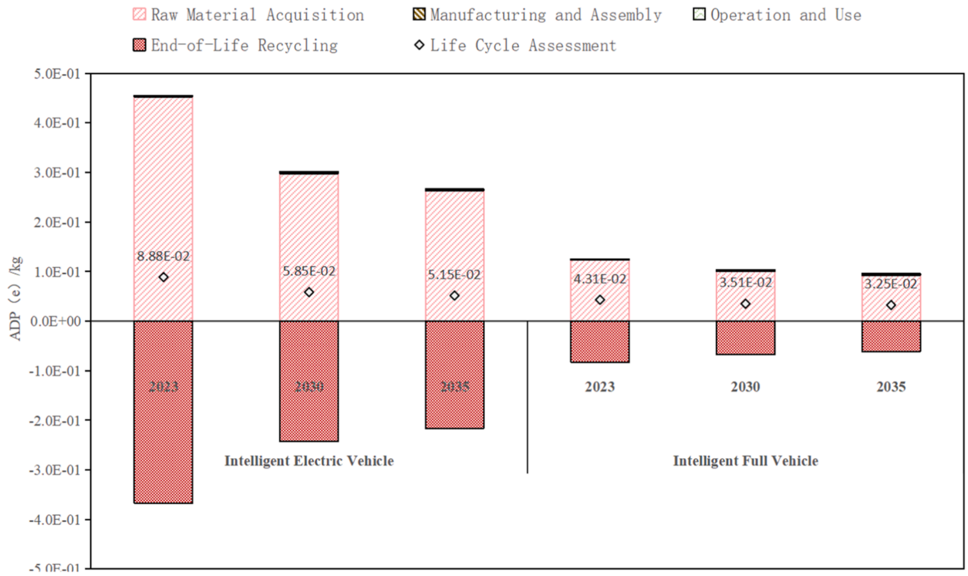

Fig. 15. The consumption of mineral resources for the full life cycle of intelligent electric vehicles and intelligent fuel vehicles for 2035.

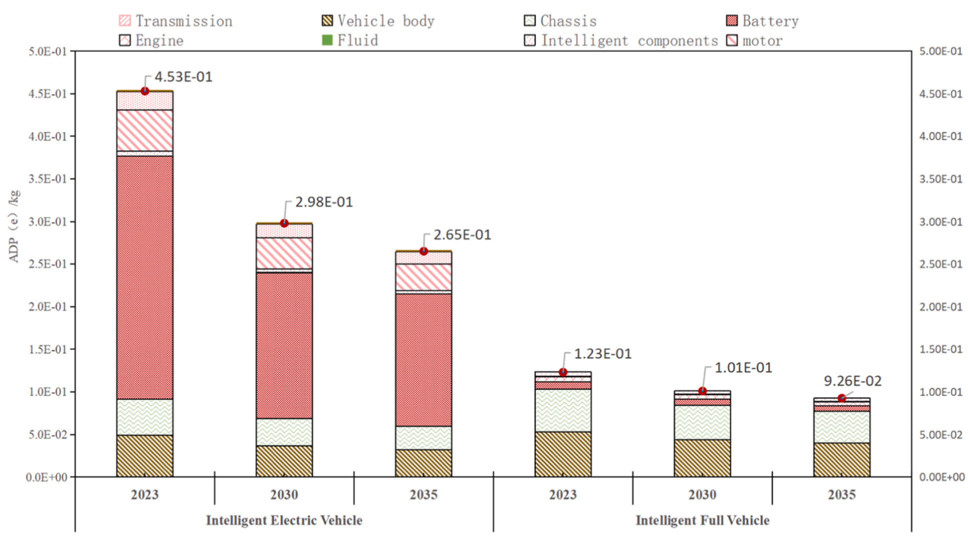

Fig. 16. Consumption of mineral resources for components of intelligent electric vehicles and intelligent fuel vehicles for 2035.

consumption of intelligent electric vehicles, efforts should continue to focus on increasing the battery energy density and reducing the consumption of copper and other metal materials in electrical control units, motors, and other components of the electric drive system.

5.2.2.2. Fossil energy consumption. The life cycle ADP(f) for intelligent electric vehicles in 2025, 2030, and 2035 were 1.95E+ 05 MJ, 1.58E+ 05 MJ, and 1.08E+ 05 MJ, respectively, representing reductions of 30.60 %, 43.77 %, and 61.57 %, respectively, compared to 2023. For intelligent fuel vehicles, the life cycle ADP(f) in 2025, 2030, and 2035 were 3.48E+ 05 MJ, 2.84E+ 05 MJ, and 2.00E+ 05 MJ, respectively, representing reductions of 27.20 %, 40.59 %, and 57.53 %, respectively, compared with 2023. The life cycle fossil energy consumption ADP(f) for intelligent electric vehicles and intelligent fuel vehicles towards 2035 is shown in Fig. 17.

The analysis of Fig. 17 reveals that the operation and manufacturing/assembly stages contribute significantly to the reduction in life cycle fossil energy consumption for both intelligent electric vehicles and intelligent fuel vehicles. For intelligent electric vehicles, fossil energy consumption during the operation stage in 2025, 2030, and 2035 decreased by 33.33 %, 46.85 %, and 66.98 %, respectively, compared with that in 2023. The fossil energy consumption during the manufacturing/assembly stage decreased by 27.14 %, 41.75 %, and 58.41 %, respectively. For intelligent fuel vehicles, these reductions were 29.70 %, 42.89 %, and 60.41 % during the operation stage and 18.15 %, 33.14 %, and 50.89 % during the manufacturing/assembly stage, respectively. A comparative analysis of the life cycle fossil energy consumption of intelligent electric vehicles and intelligent fuel vehicles shows that, compared to intelligent fuel vehicles, the fossil energy consumption of intelligent electric vehicles decreased by 43.97 %, 44.37 %, and 46.00 % by 2025, 2030, and 2035, respectively.

5.2.2.3. Carbon emissions. The life cycle carbon emissions of intelligent electric vehicles in 2025, 2030, and 2035 were 1.99E+ 04 kg, 1.62E+ 04 kg, and 1.14E+ 04 kg, respectively, representing reductions of 31.14 %, 43.94 %, and 60.55 %, respectively, compared to 2023. For intelligent fuel vehicles, the life-cycle carbon emissions in 2025, 2030, and 2035 were 2.79E+ 04 kg, 2.28E+ 04 kg, and 1.62E+ 04 kg, respectively, representing reductions of 27.15 %, 40.47 %, and 57.75 %, respectively, compared with 2023. The life cycle GWP of intelligent

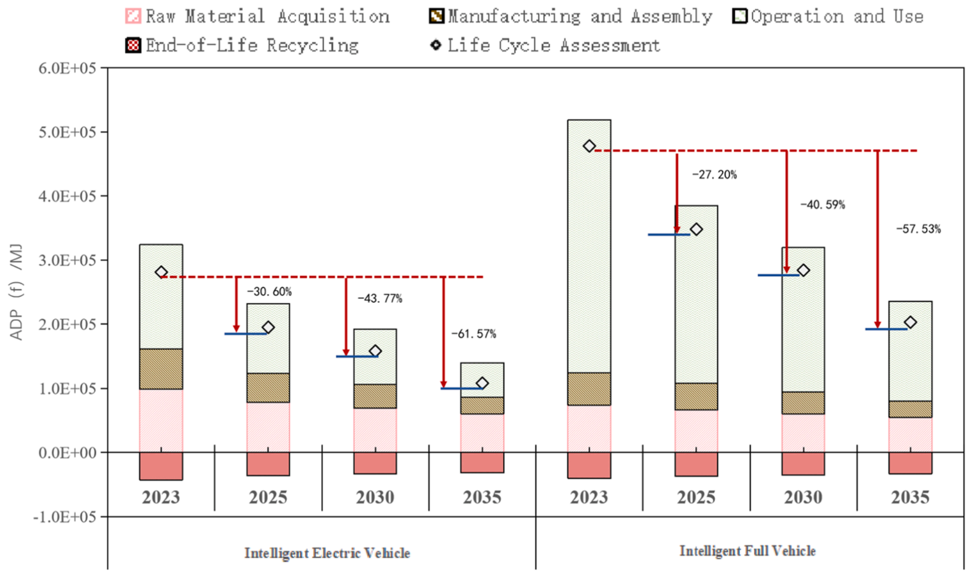

Fig. 17. Fossil energy consumption for the full life cycle of intelligent electric vehicles and intelligent fuel vehicles for 2035.

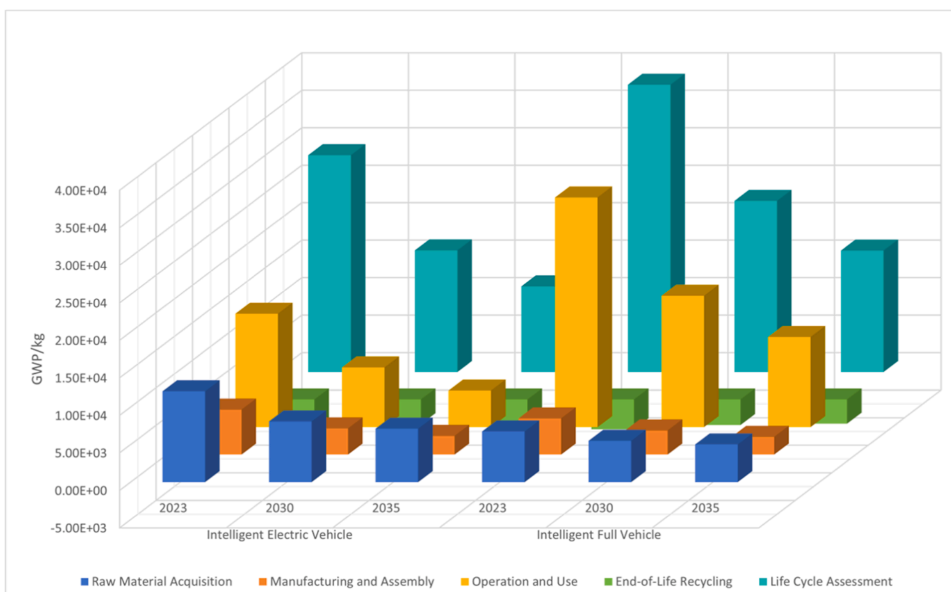

Fig. 18. The full life cycle carbon emissions of intelligent electric vehicles and intelligent fuel vehicles for 2035.

electric and fuel vehicles by 2035 are shown in Fig. 18.

The analysis of Fig. 18 reveals that the operation stage contributes significantly to a reduction in the life cycle carbon emissions for both intelligent electric vehicles and intelligent fuel vehicles. For intelligent electric vehicles, carbon emissions during the operation stage in 2025, 2030, and 2035 decreased by 33.84 %, 47.35 %, and 67.81 %, respectively, compared with those in 2023. For intelligent fuel vehicles, the reductions were 29.74 %, 42.81 %, and 60.78 %. A comparative analysis of the life cycle carbon emissions of intelligent electric vehicles and intelligent fuel vehicles showed that, compared to intelligent fuel vehicles, the carbon emissions of intelligent electric vehicles decrease by 28.67 %, 28.95 %, and 29.54 % in 2025, 2030, and 2035, respectively.

5.2.2.4. Pollutant emissions. The life cycle acidification potential(AP) of intelligent electric vehicles and intelligent fuel vehicles towards 2035 are shown in Fig. 19. The life cycle AP for intelligent electric vehicles in 2025, 2030, and 2035 were 4.62E+ 01 kg, 3.81E+ 01 kg, and 2.74E+ 01 kg, respectively, representing reductions of 30.94 %, 43.05 %, and 59.04 %, respectively, compared with 2023. For intelligent fuel vehicles, the life cycle AP in 2025, 2030, and 2035 were 3.50E+ 01 kg, 2.89E+ 01 kg, and 2.14E+ 01 kg, respectively, representing reductions of 24.08 %, 37.31 %, and 53.58 %, respectively, compared with 2023. The analysis of Fig. 18 reveals that the raw material acquisition and operation stages contributed the most to the reduction in the life cycle AP for both intelligent electric vehicles and intelligent fuel vehicles. For intelligent electric vehicles, the AP during the raw material acquisition stage in 2025, 2030, and 2035 decreased by 25.25 %, 33.40 %, and 41.14 %, respectively, compared with that in 2023. The AP during the operation stage decreases by 33.75 %, 47.32 %, and 67.82 %, respectively. For intelligent fuel vehicles, the reductions were 10.00 %, 18.40 %, and 25.20 % during the raw material acquisition stage and 29.54 %, 42.70 %, and 60.50 % during the operation stage. A comparative analysis of the life cycle AP of intelligent electric vehicles and intelligent fuel vehicles shows that compared to intelligent

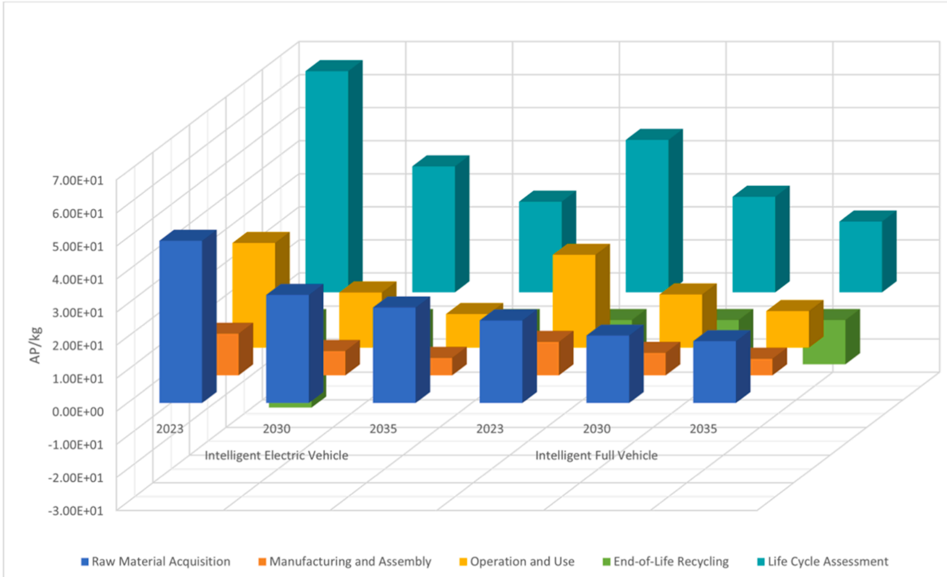

Fig. 19. The full life cycle acidizing potential of intelligent electric vehicles and intelligent fuel vehicles for 2035.

fuel vehicles, the AP of intelligent electric vehicles increases by 32.00 %, 31.83 %, and 28.04 % in 2025, 2030, and 2035, respectively, showing a significant decrease from 45.12 % in 2023. This demonstrates that, with the reduction in electricity consumption and advancements in vehicle lightweighting technology, the gap in the acidification potential between intelligent electric vehicles and intelligent fuel vehicles is gradually narrowing.

The life cycle eutrophication potential (EP) of intelligent electric and fuel vehicles towards 2035 is shown in Fig. 20. The life cycle EP for intelligent electric vehicles in 2025, 2030, and 2035 were 5.07E+ 00 kg, 4.08E+ 00 kg, and 2.74E+ 00 kg, respectively, representing reductions of 31.02 %, 44.49 %, and 62.76 %, respectively, compared to 2023. For intelligent fuel vehicles, the life cycle EP in 2025, 2030, and 2035 were 4.55E+ 00 kg, 3.74E+ 00 kg, and 2.71E+ 00 kg, respectively, representing reductions of 31.02 %, 38.59 %, and 55.50 %, respectively, compared with 2023. The analysis of Fig. 19 reveals that the operation stage contributes the most to the reduction in the life cycle EP for both intelligent electric and fuel vehicles. For intelligent electric vehicles, the EP during the operation stage in 2025, 2030, and 2035 decreased by 34.02 %, 47.36 %, and 67.82 %, respectively, compared with that in 2023. For intelligent fuel vehicles, the reductions were 29.68 %, 42.64 %, and 60.35 %, respectively. A comparative analysis of the life cycle EP of intelligent electric vehicles and intelligent fuel vehicles shows that compared to intelligent fuel vehicles, the EP of intelligent electric vehicles increases by 11.43 %, 9.09 %, and 1.11 % in 2025, 2030, and 2035, respectively, showing a significant decrease from the 20.69 % increase in 2023. This further demonstrates the energy-saving and emission reduction potentials of intelligent electric vehicles.

The life cycle photochemical ozone creation potential (POCP) of intelligent electric vehicles and intelligent fuel vehicles towards 2035 is

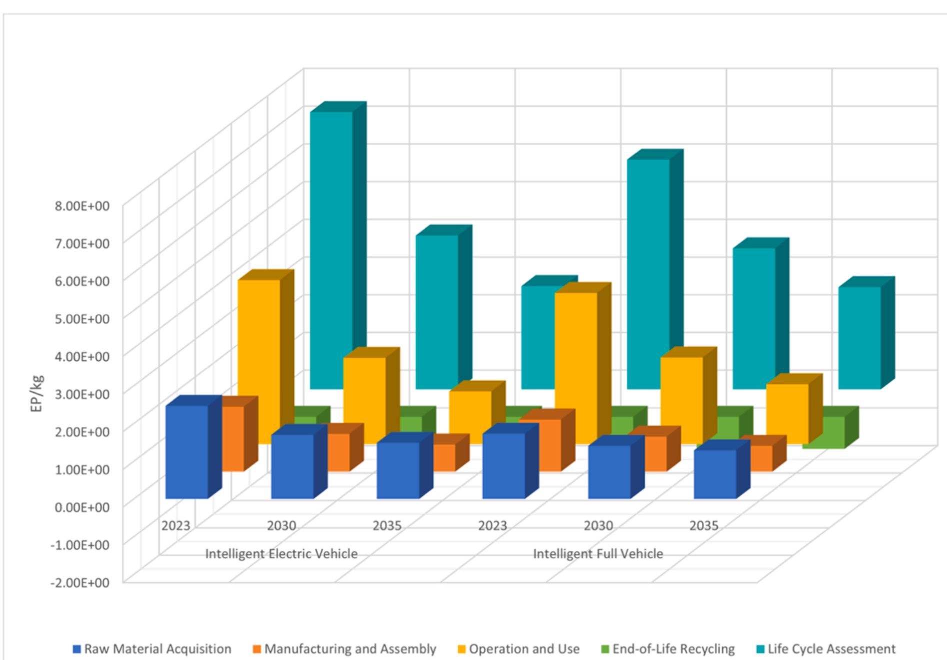

Fig. 20. The eutrophication potential of the whole life cycle of intelligent electric vehicles and intelligent fuel vehicles for 2035.

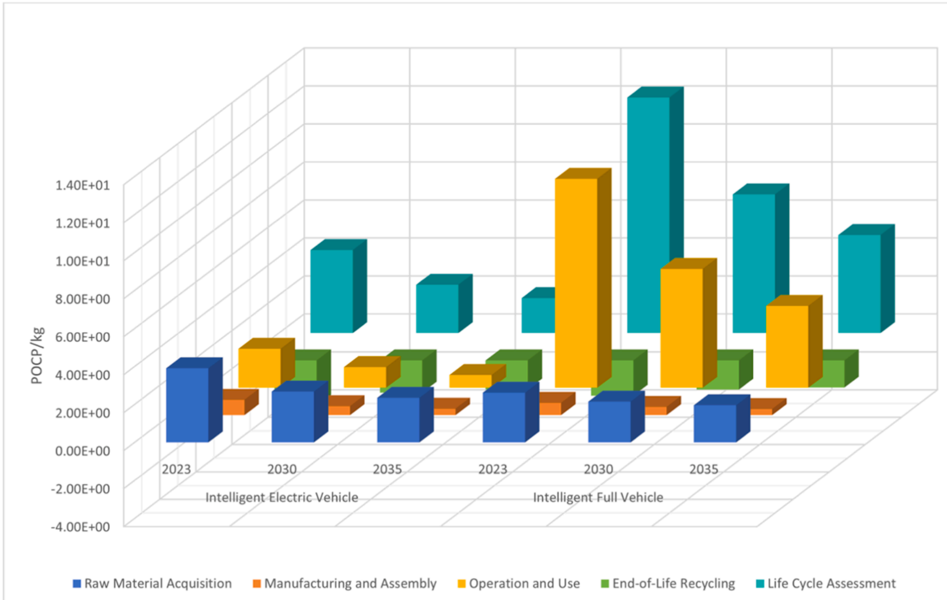

Fig. 21. Full life cycle photochemical smog potential of intelligent electric vehicles and intelligent fuel vehicles for 2035.

shown in Fig. 21. The life cycle POCP for intelligent electric vehicles in 2025, 2030, and 2035 were 3.08E+ 00 kg, 2.54E+ 00 kg, and 1.84E+ 00 kg, respectively, representing reductions of 29.52 %, 41.88 %, and 57.89 %, respectively, compared to 2023. For intelligent fuel vehicles, the life cycle POCP in 2025, 2030, and 2035 were 8.92E+ 00 kg, 7.30E+ 00 kg, and 5.16E+ 00 kg, respectively, representing reductions of 28.06 %, 41.13 %, and 58.39 %, respectively, compared with 2023.

The analysis of Fig. 21 reveals that the operation stage contributes the most to the reduction in the life cycle POCP for both intelligent electric and fuel vehicles. For intelligent electric vehicles, the POCP during the operation stage in 2025, 2030, and 2035 decreased by 33.66 %, 46.83 %, and 66.98 %, respectively, compared with that in 2023. For intelligent fuel vehicles, the reductions were 29.82 %, 43.09 %, and 60.82 %, respectively. A comparative analysis of the life cycle POCP of intelligent electric vehicles and intelligent fuel vehicles shows that compared to intelligent fuel vehicles, the POCP of intelligent electric vehicles decreased by 65.47 %, 65.21 %, and 64.34 % in 2025, 2030, and 2035, respectively.

The life cycle ozone depletion potential (ODP) of intelligent electric vehicles and intelligent fuel vehicles towards 2035 is shown in Fig. 22. In 2025, 2030, and 2035, the life cycle ODP of both intelligent electric vehicles and intelligent fuel vehicles showed an increasing trend. This is primarily because of the continuous growth in the proportion of solar power in the energy mix, as solar power generation can increase ozone layer depletion. For intelligent electric vehicles, the ODP increased by 5.08 %, 31.64 %, and 62.89 % in 2025, 2030, and 2035, respectively. For intelligent fuel vehicles, the ODP increased by 24.51 %, 58.12 %, and 117.53 %. A comparative analysis of the life cycle ODP of intelligent electric vehicles and intelligent fuel vehicles shows that, compared to

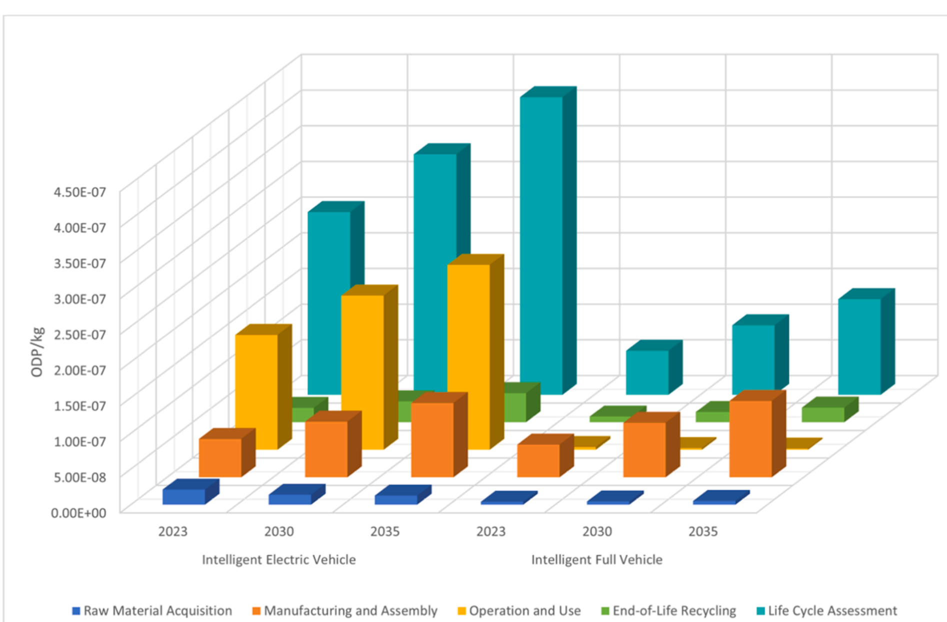

Fig. 22. The ozone layer loss potential for the whole life cycle of intelligent electric vehicles and intelligent fuel vehicles for 2035.

intelligent fuel vehicles, the ODP of intelligent electric vehicles increased by 250.72 %, 246.00 %, and 211.19 % in 2025, 2030, and 2035, respectively. This shows a significant decrease from the 315.58 % increase in 2023, further demonstrating the energy-saving and emission reduction potential of intelligent electric vehicles.

6. Conclusion and prospect

6.1. Conclusion

1. Compared with intelligent fuel vehicles, intelligent electric vehicles demonstrated multiple advantages in terms of pollutant emissions. In life cycle assessments, ADP(f), GWP, and POCP of intelligent electric vehicles were significantly lower than those of intelligent fuel vehicles. Notably, the advantages of intelligent electric vehicles in POCP highlight their potential as clean energy transportation tools, providing an important pathway and direction for achieving sustainable development goals.
2. Two scenarios were constructed based on intelligence and connectivity: single-vehicle intelligence coupled with multiple operational scenarios, and vehicle-road coordination coupled with multiple operational scenarios. A scenario simulation was used to quantitatively analyze and compare the impact of key intelligence and connectivity factors on the energy-saving and emission reduction potential of electric vehicles and fuel vehicles. The results showed that single-vehicle intelligence and vehicle-road coordination technologies can effectively reduce the life cycle energy consumption and emissions of both electric and fuel vehicles, with a greater reduction in intelligent electric vehicles. As the level of single-vehicle intelligence increases, the energy-saving and emission reduction performance of electric vehicles also improves compared to fuel vehicles. In urban road scenarios, L2-L3 level electric vehicles equipped with vehicle-road coordination technology reduce life cycle carbon emissions by 20.22 %-22.35 % compared to the L1 level, whereas fuel vehicles reduce by 15.77 %-19.58 %. In highway scenarios, L2-L3 level electric vehicles reduce life cycle carbon emissions by 12.29 %-14.50 % compared to the L1 level, while fuel vehicles reduce by 3.47 %-5.91 %. Comparative analysis revealed that in urban road scenarios, L2-L3 level electric vehicles with vehicle-road coordination technology reduced life cycle carbon emissions by approximately 46 % compared to fuel vehicles and by approximately 7.5 % in highway scenarios.
3. Regional differences in the electrification scenarios of intelligent vehicles were constructed based on electrification, and scenario simulations were used to quantitatively analyze and compare the impact of regional differences on the energy-saving and emission reduction potential of intelligent electric vehicles. The results show that the life cycle assessment results for intelligent electric vehicles in North China and Southwest China were the highest and lowest, respectively. Compared to the life cycle carbon emissions based on the national power structure, the emissions in Southwest and South China decreased by 41.87 % and 10.38 %, respectively, while those in North, Central, East, Northeast, and Northwest China increased by 21.11 %, 3.81 %, 13.15 %, 9.34 %, and 6.23 %, respectively. Compared to intelligent fuel vehicles, during the operation stage, the carbon emissions of intelligent electric vehicles in North, Central, South, East, Northeast, Northwest, and Southwest China decreased by 37.25 %, 48.37 %, 57.52 %, 42.48 %, 44.77 %, 46.73 %, and 77.32 %, respectively. Therefore, the cleaner the power structure, the greater the energy-saving and emission reduction benefits of intelligent electric vehicles.
4. Based on key factors such as lightweighting, battery energy density, power structure, and energy consumption per 100 km, a predictive assessment and comparative study of the life cycle of intelligent electric vehicles and intelligent fuel vehicles towards 2035 was conducted. The results show that by 2035, the ADP(e), ADP(f), GWP, AP, EP, and POCP of intelligent electric vehicles are expected to decrease by 42 %, 61.57 %, 67.81 %, 59.04 %, 62.76 %, and 57.89 %, respectively, compared to 2023, whereas the ODP increases by 62.89 %. For intelligent fuel vehicles, these values decreased by 24.59 %, 57.53 %, 60.78 %, 53.58 %, 52.5 %, and 58.39 %, respectively, whereas the ODP increased by 117.53 %. By 2035, the life cycle carbon emissions of intelligent electric vehicles are expected to be 30 % lower than those of intelligent fuel vehicles. Based on the normalized results, the overall environmental impact of intelligent electric vehicles in 2035 is expected to decrease by 60.09 %, compared with a 57.39 % reduction for intelligent fuel vehicles, making the impact of intelligent electric vehicles 28.97 % lower than that of intelligent fuel vehicles. With advancements in lightweighting, battery technology, and energy consumption per 100 km, combined with an increasing proportion of clean energy in the power mix, the energy-saving and emission reduction efficiency of intelligent electric vehicles will continue to improve.

6.2. Prospect

Due to the limitations of current life cycle assessment theory and methods, as well as factors such as localization of modeling software databases and missing inventory data, coupled with the rapid evolution of intelligent and networked technologies, high-level autonomous driving has not yet been put into large-scale production, and related products are in the testing stage, lacking intuitive and accurate energy-saving and emission reduction values and application scenario research, there is a certain difference between the evaluation results of this article and actual data. Therefore, the following research prospects are proposed:

1. Improve the construction of an intelligent electric vehicle life cycle assessment model based on the entire industry chain. On the basis of the existing model, further refine the boundary and data list of the intelligent electric vehicle system, especially the analysis of the scrapped and recycled stages and hierarchical utilization scenarios of power batteries. Focus on building a full life cycle information traceability platform for key components such as power batteries, a manufacturing and assembly process data management platform, and a vehicle operation and use energy consumption data monitoring and management platform to achieve intelligent electric vehicle data traceability management based on the entire industry chain. Finally, construct a complete theoretical model, accurate data list, and real-time dynamic update of the full life cycle evaluation system that meets the development needs of the intelligent electric vehicle industry.
2. Expand the research on the energy-saving and emission reduction performance of intelligent electric vehicles throughout their life cycle for multiple application scenarios. The current intelligent electric vehicles equipped with advanced autonomous driving (L4, L5) are only tested and operated in limited areas and specific scenarios. The research on their intelligent and networked energy-saving and emission reduction mechanisms is not yet perfect. In the future, the full life cycle assessment method should be combined with simulation testing of intelligent vehicles in multiple scenarios such as closed parks and shared transportation, as well as actual road testing in experimental areas, in order to further verify and evaluate the energy-saving and emission reduction potential of intelligent electric vehicles in various scenarios.

CRediT authorship contribution statement

Yisong Chen: Writing – review & editing, Supervision, Software, Investigation. **Yunxiang Xing:** Project administration, Data curation. **Longxin Gao:** Formal analysis, Data curation. **Qinyang Liu:** Methodology, Investigation, Data curation, Conceptualization. **Shuo Zhang:**

Visualization, Resources. **Yongtao Liu:** Writing – original draft, Supervision.

Declaration of Competing Interest

The authors declare that they have no known competing financial interests or personal relationships that could have appeared to influence the work reported in this paper.

Acknowledgements

This research was funded by the National Key R&D Program of China (2021YFE0192900 and 2021YFB2501202), the Humanities and Social Sciences Youth Fund of the Ministry of Education (18YJCZH110), the Natural Science Foundation of the Shaanxi Province (2023-JC-QN-0664 and 2024JC-YBQN-0479), the Key Research and Development Program of the Shaanxi Province (2023JBGS-13), the Major Scientific and Technological Special Project in Shaanxi Province (2020zdzx06–01–01), and the Fundamental Research Funds for the Central Universities (300102223204).

Data availability

Data will be made available on request.

References

Abro, G.E.M., Zulkifli, S.A.B., Kumar, K., et al., 2023. Comprehensive review of recent advancements in battery technology, propulsion, power interfaces, and vehicle network systems for intelligent autonomous and connected electric vehicles. Energies 16 (6), 2925. https://doi.org/10.3390/en16062925.

Ahmadi, P., Khoshnevisan, A., 2022. Dynamic simulation and life cycle assessment of hydrogen fuel cell electric vehicles considering various hydrogen production methods. Int. J. Hydrog. Energy 47 (62), 26758–26769. https://doi.org/10.1016/j.ijhydene.2022.06.215.

Alrifaee, B., Jodar, J.G., Abel, D., 2015. Decentralized predictive cruise control for energy saving in REEV using V2I information for multiple-vehicles. IFAC-Pap. 48 (15), 320–327. https://doi.org/10.1016/j.ifacol.2015.10.046.

Amini, M.R., Gong, X., Feng, Y., et al., (2019, July). Sequential optimization of speed, thermal load, and power split in connected HEVs. In 2019 American Control Conference (ACC) (pp. 4614-4620). IEEE. ⟨https://doi.org/10.23919/acc.2019.8815158⟩.

Andersson, Ö., Börjesson, P., 2021. The greenhouse gas emissions of an electrified vehicle combined with renewable fuels: Life cycle assessment and policy implications. Appl. Energy 289, 116621. https://doi.org/10.1016/j.apenergy.2021.116621.

Bertoni, Guanetti, L., Basso, J., Masoero, M., et al., 2017. An adaptive cruise control for connected energy-saving electric vehicles. IFAC-Pap. 50 (1), 2359–2364. https://doi.org/10.1016/j.ifacol.2017.08.425.

Chen, Y., Hao, Z., Lan, L., et al., 2022. Research on energy saving and carbon reduction evaluation of the whole life cycle of pure electric vehicles with different power batteries (in Chinese). J. Automot. Eng. 04, 517–527. https://doi.org/10.3969/j.issn.2095?1469.2022.04.15.

Chen, Y., Lan, L., Du, Y., et al., 2023. Assessment of EREV / BEV / ICEV based on whole life cycle evaluation theory (in Chinese). J. Environ. Sci. (02), 516–527. https://doi.org/10.13671/j.hjkxxb.2022.0226.

Chu, L., Guo, B., Gao, H., et al., 2018. Predictive cruise control using high-definition map and real vehicle implementation. IEEE Trans. Veh. Technol. 67 (12), 11377–11389. https://doi.org/10.1109/TVT.2018.2871202.

Cui, H., Zhu, M., Xing, J., et al., 2019. Study on ACC vehicle control mode under signal intersection (in Chinese). Highw. Traffic Technol. 06, 86–93. https://doi.org/10.3969/j.issn.1002-0268.2019.06.012.

Cui, P., Zhang, J., Liu, Y., et al., 2023. Comprehensive analysis of clean fuel vehicle life cycle environment under multiple fuel scenarios. Energy 275, 127466. https://doi.org/10.1016/j.energy.2023.127466.

Ding, R., Qin, X., Dong, S., 2021. Evaluation of the remanufacturing life cycle of the electric vehicle drive motor, 1420.(in Chinese). Environ. Pollut. Prev. (11), 1410–1415. https://doi.org/10.15985/j.cnki.1001-3865.2021.11.011.

Dong, H., Yin, G., Zhuang, W., et al., 2021. Economic cruise speed optimization of connected electric vehicles based on iterative dynamic planning (in Chinese). J. Mech. Eng. 06, 121–130. https://doi.org/10.3901/JME.2021.06.121.

Fu, P., Lan, L., Chen, Y., et al., 2023. Forecast and evaluation of carbon emissions in the whole life cycle of energy-saving and new energy vehicles for 2035 (in Chinese). Environ. Sci. 04, 2365–2374. https://doi.org/10.13227/j.hjkx.202208236.

Guo, G., 2016. Vehicle collaborative control in intelligent transportation systems. National Machinery Industry Press (in Chinese).

Guo, J., Li, W., Wang, J., Luo, Y., Li, K., 2021. Safe and energy-efficient car-following control strategy for intelligent electric vehicles considering regenerative braking. IEEE Trans. Intell. Transp. Syst. 23 (7), 7070–7081. https://doi.org/10.1109/tits.2021.3066611.

Guo, L., (2019). Real-time optimization control and real vehicle verification for intelligent energy-saving vehicles (dissertation, Jilin University). Dr. (in Chinese).

Guo, X., Sun, Y., Ren, D., 2023. Life cycle carbon emission and cost-effectiveness analysis of electric vehicles in China. Energy Sustain. Dev. 72, 1–10. https://doi.org/10.1016/j.esd.2022.11.008.

Hao, H., Mu, Z., Jiang, S., et al., 2017. GHG Emissions from the production of lithium-ion batteries for electric vehicles in China. Sustainability 9 (4), 504. https://doi.org/10.3390/su9040504.

Hao, Z., (2023). Master of Full Life Cycle Evaluation and Step Utilization Research of Vehicle Power Battery (dissertation, Chang'an University). Master of Arts. (in Chinese).

Hauschild, M.Z., Rosenbaum, R.K., Olsen, S.I., 2018. Life cycle assessment, 2018. Springer International Publishing, Cham. ⟨https://doi.org/10.1007/978-3-319-56475-3⟩.

Jia, Y., Jibrin, R., Görges, D., 2020. Energy-optimal adaptive cruise control for electric vehicles based on linear and nonlinear model predictive control. IEEE Trans. Veh. Technol. 69 (12), 14173–14187. https://doi.org/10.1109/tvt.2020.3044265.

Jin, H., Ding, F., 2018. Study on economic speed of intelligent vehicle lane, 553. (in Chinese). Automot. Eng. 05, 542–546. https://doi.org/10.19562/j.chinasae.qcgc.2018.05.007.

Jo, B.U., Ahn, J., 2022. Optimal staging of reusable launch vehicles for minimum life cycle cost. Aerosp. Sci. Technol. 127, 107703. https://doi.org/10.1016/j.ast.2022.107703.

Joshi, A., Sharma, R., Baral, B., 2022. Comparative life cycle assessment of conventional combustion engine vehicle, battery electric vehicle and fuel cell electric vehicle in Nepal. J. Clean. Prod. 379, 134407. https://doi.org/10.1016/j.jclepro.2022.134407.

Jujjavarapu, S., Kota, S., Kotkunde, N.R., et al., (2023). Life cycle assessment study on glove box assembly of Indian passenger vehicles. Proceedings of the Institution of Mechanical Engineers, Part E: Journal of Process Mechanical Engineering, 09544089231215200. ⟨https://doi.org/10.1177/09544089231215200⟩.

Lai, X., Chen, Q., Tang, X., et al., 2022. Critical review of life cycle assessment of lithium-ion batteries for electric vehicles: a lifespan perspective. Etransportation 12, 100169. https://doi.org/10.1016/j.etran.2022.100169.

Li, H., Zhang, J., Sun, X., et al., 2022. A survey of vehicle group behaviors simulation under a connected vehicle environment. Phys. A: Stat. Mech. its Appl. 603, 127816. https://doi.org/10.1016/j.physa.2022.127816.

Li, J., (2015). Master of Life Cycle Evaluation and Analysis of pure Electric Vehicle and Fuel Vehicle PowerSystem (dissertation, Hunan University). Master of Arts.

Li, X., Wang, Z., Zhang, L., et al., 2023. Electric vehicle behavior modeling and applications in vehicle-grid integration: An overview. Energy 268, 126647. https://doi.org/10.1016/j.energy.2023.126647.

Liao, G., Zheng, L., Zhang, Z., et al., 2022. Study on the optimal speed planning and collision avoidance control of electric vehicles considering the signal light state (in Chinese). Chin. Sci.: Tech. Sci. (07), 1134–1144. https://doi.org/10.1360/SST-2021-0133.

Liu, K., (2016). BYD E6 Master of full life cycle Evaluation (dissertation, Fujian Agriculture and Forestry University). Master of Arts (in Chinese).

Liu, K., Xu, X., 2016. Research progress in the life cycle evaluation of electric vehicles, 136 (in Chinese). Mech. Electr. Technol. 01, 127–131. https://doi.org/10.3969/j.issn.1672-4801.2016.01.039.

Luo, K., (2020). Research on economic cruise distributed control of intelligent Connected Electric vehicle queue (Master's thesis, Southeast University). (in Chinese).

Ma, J., (2019). Master of full life cycle evaluation research of pure electric vehicles with different power batteries (thesis, Chang'an University). Master of Arts.

Madhusudhanan, A.K., Na, X., 2020. Effect of a traffic speed based cruise control on an electric vehicle' s performance and an energy consumption model of an electric vehicle. IEEE/CAA J. Autom. Sin. 7 (2), 386–394. https://doi.org/10.1109/jas.2020.1003030.

Martyushev, N.V., Malozyomov, B.V., Sorokova, S.N., et al., 2023. Mathematical modeling the performance of an electric vehicle considering various driving cycles. Mathematics 11 (11), 2586. https://doi.org/10.3390/math11112586.

Meng, X., Liu, Q., Yang, J., et al., 2022. Estimation method of waste tire production in China and its uncertainty. Renew. Resour. Circ. Econ. (02), 21–26 (in Chinese).

Naranjo, G.P.S., Bolonio, D., Ortega, M.F., et al., 2021. Comparative life cycle assessment of conventional, electric and hybrid passenger vehicles in Spain. J. Clean. Prod. 291, 125883. https://doi.org/10.1016/j.jclepro.2021.125883.

Obaid, L., Alattieh, S.A., Abdallah, M., et al., 2023. Environmental impacts of the transition to automated vehicles: A life cycle perspective. Sustain. Mater. Technol. 38, e00725. https://doi.org/10.1016/j.susmat.2023.e00725.

Ojeda, L.L., Han, J., Sciarretta, A., De Nunzio, G., et al., (2017, December). A real-time eco-driving strategy for automated electric vehicles. In 2017 IEEE 56th annual conference on decision and control (CDC) (pp. 2768-2774). IEEE. ⟨https://doi.org/10.1109/cdc.2017.8264061⟩.

Pan, X., Chen, B., Timotheou, S., et al., 2022. A convex optimal control framework for autonomous vehicle intersection crossing. IEEE Trans. Intell. Transp. Syst. 24 (1), 163–177. https://doi.org/10.1109/tits.2022.3211272.

Paredes, J.F., Cazar, G.P., Donkers, M.C.F., 2019. A shrinking horizon approach to eco-driving for electric city buses: implementation and experimental results. IFAC-Pap. 52 (5), 556–561. https://doi.org/10.1016/j.ifacol.2019.09.088.

Peng, T., Ren, L., Ou, X., 2023. Development and application of life-cycle energy consumption and carbon footprint analysis model for passenger vehicles in China. Energy 282, 128412. https://doi.org/10.1016/j.energy.2023.128412.

Qiao, Q., Zhao, F., Liu, Z., et al., 2017. Cradle-to-gate greenhouse gas emissions of battery electric and internal combustion engine vehicles in China. Appl. Energy 204, 1399–1411. https://doi.org/10.1016/j.apenergy.2017.05.041.
Quan, J., Zhao, S., Song, D., et al., 2022. Comparative life cycle assessment of LFP and NCM batteries including the secondary use and different recycling technologies. Sci. Total Environ. 819, 153105. https://doi.org/10.1016/j.scitotenv.2022.153105.
Rammohan, A., 2023. Revolutionizing Intelligent Transportation Systems with Cellular Vehicle-to-Everything (C-V2X) technology: current trends, use cases, emerging technologies, standardization bodies, industry analytics and future directions. Veh. Commun., 100638 https://doi.org/10.1016/j.vehcom.2023.100638.
Sato, F.E.K., Nakata, T., 2021. Analysis of the impact of vehicle lightweighting on recycling benefits considering life cycle energy reductions. Resour., Conserv. Recycl. 164, 105118. https://doi.org/10.1016/j.resconrec.2020.105118.
Shafique, M., Azam, A., Rafiq, M., et al., 2022. Life cycle assessment of electric vehicles and internal combustion engine vehicles: a case study of Hong Kong. Res. Transp. Econ. 91, 101112. https://doi.org/10.1016/j.retrec.2021.101112.
Shen, D., Karbowski, D., Rousseau, A., 2020. A minimum principle-based algorithm for energy-efficient eco-driving of electric vehicles in various traffic and road conditions. IEEE Trans. Intell. Veh. 5 (4), 725–737. https://doi.org/10.1109/tiv.2020.3011055.
Song, X., Deng, C., Shen, P., et al., 2023. Environmental impact and carbon footprint analysis of pure electric vehicles based on life cycle evaluation (in Chinese). Environ. Sci. Res. 11, 2179–2188. https://doi.org/10.13198/j.issn.1001-6929.2023.08.15.
Tagliaferri, C., Evangelisti, S., Acconcia, F., et al., 2016. Life cycle assessment of future electric and hybrid vehicles: a cradle-to-grave systems engineering approach. Chem. Eng. Res. Des. 112, 298–309. https://doi.org/10.1016/j.cherd.2016.07.003.
The Chinese Society of Automotive Engineering. (2020). Energy-saving and new energy vehicle technology Roadmap 2.0. (in Chinese).
Verma, S., Dwivedi, G., Verma, P., 2022. Life cycle assessment of electric vehicles in comparison to combustion engine vehicles: a review. Mater. Today.: Proc. 49, 217–222. https://doi.org/10.1016/j.matpr.2021.01.666.
Wang, J., Zhu, K., Hossain, E., 2021. Green Internet of Vehicles (IoV) in the 6G era: toward sustainable vehicular communications and networking. IEEE Trans. Green. Commun. Netw. 6 (1), 391–423. https://doi.org/10.1109/tgcn.2021.3127923.
Wang, J., Liu, X., Mei, W., et al., 2023. Regional carbon emission assessment of electric vehicles from the full life cycle perspective (in Chinese). Electr. Power Constr. 06, 33–40. https://doi.org/10.12204/j.issn.1000-7229.2023.06.004.
Wang, Q., Xue, M., Lin, B., et al., 2020. Well-to-wheel analysis of energy consumption, greenhouse gas and air pollutants emissions of hydrogen fuel cell vehicle in China. J. Clean. Prod. 275, 123061. https://doi.org/10.1016/j.jclepro.2020.123061.
Wang, Y., Guo, G., 2019. Collaborative optimization control of vehicle speed and traffic signal at urban intersections. Control Decis. Mak. 34 (11), 2397–2406 (in Chinese).
Wang, Z., (2018). Master of power battery recycling potential and Life Cycle Evaluation of new energy vehicles (thesis, Tsinghua University). Master of Arts (in Chinese).
Wei, Z., Hao, P., Barth, M.J., (2019, June). Developing an adaptive strategy for connected eco-driving under uncertain traffic condition. In 2019 IEEE Intelligent Vehicles Symposium (IV) (pp. 2066-2071). IEEE. ⟨https://doi.org/10.1109/ivs.2019.8813819⟩.
Xia, X., Li, P., Xia, Z., et al., 2022. Life cycle carbon footprint of electric vehicles in different countries: a review. Sep. Purif. Technol. 301, 122063. https://doi.org/10.1016/j.seppur.2022.122063.
Yang, L., Chen, H., Li, H., et al., 2023. Life cycle water footprint of electric and internal combustion engine vehicles in China. Environ. Sci. Pollut. Res. 30 (33), 80442–80461. https://doi.org/10.1007/s11356-023-28002-0.
Yang, Y., (2021). Research on ecological collaborative adaptive cruise control strategy of connected vehicle queue (Doctoral dissertation, Changchun: Jilin University). (in Chinese).
Yang, Y., Zhao, Y., Hao, Z., et al., 2022. Research on the performance evaluation of energy saving and emission reduction in the whole life cycle of intelligent and connected vehicles (in Chinese). Chin. Highw. J. 05, 266–274. https://doi.org/10.19721/j.cnki.1001-7372.2022.05.025.
Yu, R., Cong, L., Hui, Y., et al., 2022. Life cycle CO2 emissions for the new energy vehicles in China drawing on the reshaped survival pattern. Sci. Total Environ. 826, 154102. https://doi.org/10.1016/j.scitotenv.2022.154102.
Zhang, J., Dong, S., Li, Z., et al., 2019. An eco-driving signal control model for divisible electric platoons in cooperative vehicle-infrastructure systems. IEEE Access 7, 83277–83285. https://doi.org/10.1109/access.2019.2922227.
Zhang, X., Fang, S., Shen, Y., et al., 2023. Hierarchical velocity optimization for connected automated vehicles with cellular vehicle-to-everything communication at continuous signalized intersections. IEEE Trans. Intell. Transp. Syst. https://doi.org/10.1109/TITS.2023.3274580.
Zhao, Z., Shao, C., Chen, J., 2021. Evaluation of the carbon emission reduction effect of the whole life cycle of provincial private electric vehicles in China (in Chinese). Environ. Sci. Res. 09, 2076–2085. https://doi.org/10.13198/j.issn.1001-6929.2021.05.09.
Zheng, Y., Li, S.E., Li, K., et al., 2015. Stability margin improvement of vehicular platoon considering undirected topology and asymmetric control. IEEE Trans. Control Syst. Technol. 24 (4), 1253–1265. https://doi.org/10.1109/tcst.2015.2483564.
Zhou, Boya., (2016). Energy consumption, carbon emissions and cost and benefits of the life cycle of electric vehicles (thesis, Tsinghua University). Dr. (in Chinese).

Further reading

Zhang, H., Zhao, F., Hao, H., et al., Life Cycle Emissions of Passenger Vehicles in China: A Sensitivity Analysis of Multiple Influencing Factors. Sustainability, 15(6), 4854. ⟨https://doi.org/10.3390/su15064854⟩.
Kim, M.J., Lee, E.J., Kim, C.J., et al., 2021. Life cycle assessment of LPG and diesel vehicles in Korea. Korean J. Chem. Eng. 38 (5), 938–944. https://doi.org/10.1007/s11814-021-0761-0.
Xia, X., Li, P., 2022. A review of the life cycle assessment of electric vehicles: considering the influence of batteries. Sci. Total Environ. 814, 152870. https://doi.org/10.1016/j.scitotenv.2021.152870.